Review

A Comprehensive Review of the Advances, Manufacturing, Properties, Innovations, Environmental Impact and Applications of Ultra-High-Performance Concrete (UHPC)

Gregor Kravanja [1,2], Ahmad Rizwan Mumtaz [1] and Stojan Kravanja [1,*]

1 Faculty of Civil Engineering, Transportation Engineering and Architecture, University of Maribor, Smetanova 17, 2000 Maribor, Slovenia; gregor.kravanja@um.si (G.K.); ahmadrizwan.mumtaz@student.um.si (A.R.M.)
2 Faculty of Chemistry and Chemical Engineering, University of Maribor, Smetanova 17, 2000 Maribor, Slovenia
* Correspondence: stojan.kravanja@um.si

Abstract: The article presents the progress and applications of ultra-high-performance concrete (UHPC), a revolutionary material in modern construction that offers unparalleled strength, durability, and sustainability. The overview includes the historical development of UHPC, covering its production and design aspects, including composition and design methodology. It describes the mechanical properties and durability of UHPC and highlights recent innovations and research breakthroughs. The potential integration of multifunctional properties such as self-heating, self-sensing, self-luminescence and superhydrophobicity, is explored. In addition, advances in nanotechnology related to UHPC are addressed. Beyond the actual material properties, the article presents an environmental impact assessment and a life-cycle cost analysis, providing an insight into the wider implications of using UHPC. To illustrate the environmental aspects, the determination of CO_2 emissions is explained using three numerical examples. Finally, various applications of UHPC are presented, focusing on the construction of buildings and bridges. By synthesizing the above-mentioned aspects, this review paper captures the dynamic landscape of UHPC and serves as a valuable resource for researchers and engineers in the field of construction materials.

Keywords: ultra-high-performance concrete; UHPC; manufacturing; mechanical properties; durability; multifunctionality; environmental impact assessment; life-cycle costs

1. Introduction

Ultra-high-performance concrete (UHPC) is defined as a type of concrete that exhibits compressive strength greater than 120 MPa, a nominal maximum aggregate size of less than 5 mm, and flowability between 200 mm and 250 mm [1]. UHPC exhibits a tensile strength greater than 5 MPa. According to the Federal Highway Administration (FHWA), USA, UHPC is characterized by the use of a combination of Portland cement and supplementary cementitious materials, an optimised gradation of granular materials, a high volume of discontinuous internal fibres, and a low water-to-cementitious materials ratio of less than 0.25. The microstructure of UHPC is characterized irregular pores, which control liquid evaporation and enhance durability in comparison to conventional and high-performance concretes [2].

The development of UHPC can be traced back to the early 1980s [3]. After decades of research, UHPC has emerged as a highly innovative product in the field of concrete technology, distinguished by its exceptional mechanical properties and superior durability. The service life of reinforced concrete structures is largely dependent on the durability of the concrete, and the excellent durability properties of UHPC can lead to a significant increase in service life, thus reducing maintenance costs.

In addition to its durability properties, UHPC also exhibits high flowability, allowing it to meet a wide range of structural requirements. UHPC has also been reported to possess high impermeability against carbon dioxide, chlorides, and sulphates [4]. The inclusion of steel fibres in the mix design of UHPC can further enhance its compressive and tensile strength, which can exceed 150 MPa and 20 MPa, respectively [5]. The ductility and energy absorption capacity of UHPC, due to the presence of steel fibres, are typically 300-times greater than that of high-performance concrete [6].

Workability, compressive strength, durability and economy are the key factors and priorities of conventional concrete (CC) based on the ACI mixture design method [7]. Portland cement (PC) is the main ingredient in the production of UHPC as a cementitious binder, accompanied by other supplementary cementitious materials (SCM); in most cases, silica fume (SF) is used as an SCM [8]. Mechanical consistency, maximum particle packing density and the lowest number of defects are the fundamental basis for the production of UHPC, considering both micro and macro characteristics of the design mix materials [9–11]. In addition to the micro and macro properties of the design mix materials, it is also crucial to consider the physical and chemical properties of the materials [11]. To produce UHPC with durable, viable, economical and excellent mechanical properties, it is crucial to develop scientifically efficient mix design methods [7].

Nonetheless, there are some disadvantages associated with UHPC, particularly concerning shrinkage and cracking during the early stages of concreting due to autogenous and drying shrinkage. Consequently, there has been limited research conducted on the long-term behaviour of this concrete. Additionally, UHPC is more costly than normal concrete, raising concerns about its viability when unconventional concrete can economically meet design requirements. The primary limitation to the broader utilization of UHPC is the high cost of several expensive raw materials in the mix [6].

This review article provides a comprehensive exploration of UHPC, encompassing its historical evolution, manufacturing and design processes, production methodologies, mechanical properties, recent innovations, durability aspects and environmental impact. The significance of this review lies in its holistic coverage, offering a deep dive into the multifaceted aspects of UHPC. By tracing the historical trajectory, we set the stage for understanding how UHPC has evolved from a material with extraordinary mechanical properties to a multifunctional wonder, capable of self-heating, self-sensing, self-luminescence and superhydrophobicity. The exploration extends to the critical assessment of UHPC's durability, environmental implications through life-cycle assessments, sustainable practices and life-cycle cost analyses. The review concludes with an insightful discussion on the diverse applications of UHPC and outlines future prospects. In Table 1, a comprehensive overview of several review articles published in the last decade is provided, offering a comparative analysis of their key features. Importantly, our work, as outlined in this table, is distinguished by its unique incorporation of several innovations that set it apart from its counterparts. This comprehensive overview serves as a valuable resource for researchers, engineers and practitioners in the field, offering a synthesized understanding of UHPC's journey, its current state, and the promising avenues it opens for the future of construction materials.

Table 1. Summarized overview of recent decade's review articles on UHCP.

Reviews Content	Year	References
Historical development of UHPC composition, Design methodology, Production, Manufacturing, Mechanical Properties, Innovation and research, Superhydrophobicity, Self-Sensing, Multifunctionality, Durability, Nanotechnology, Life cycle assessment, Numerical examples and Applications	2024	This review
Production, Manufacturing, Mechanical Properties, Self-sensing and Applications	2023	[12]
Design methodology, Production Manufacturing, and Mechanical Properties	2023	[13]

Table 1. *Cont.*

Reviews Content	Year	References
Mechanical Properties, Innovation and research, Superhydrophobicity, Durability and Nanotechnology	2023	[14]
Design methodology, Production, Manufacturing, Mechanical Properties, Innovation and research, and 3-D printing	2023	[15]
Design methodology, Mechanical Properties and Durability	2022	[16]
Historical development of UHP composition and Mechanical Properties	2022	[17]
Design methodology, Production and Manufacturing	2022	[18]
Historical development of UHPC composition, Mechanical Properties, Durability, Life-cycle assessment and Applications	2022	[19]
Mechanical Properties and Durability	2022	[20]
Historical development of UHPC composition, Mechanical Properties, Self-sensing, Durability and Nanotechnology	2022	[21]
Superhydrophobicity and Durability	2022	[22]
Design methodology and Production	2021	[7]
Design methodology and Mechanical Properties	2021	[23]
Mechanical Properties and Life-Cycle Assessment	2021	[24]
Historical development of UHPC composition, Design methodology, Production, Mechanical Properties, Durability and Applications	2021	[25]
Design methodology and Mechanical Properties	2020	[26]
Historical development of UHPC composition, Design methodology, Production and Applications	2018	[11]
Historical development of UHPC composition, Design methodology, Production, Manufacturing and Nanotechnology	2015	[10]

History of UHPC

Concrete is not really an invention of 20th or 21st century. Concrete, as a construction material, has been in use since ancient times, dating back to the Before Christ (BC) era. In 300 BC, Romans utilised pozzolana cement, and in 800 BC, Greeks employed lime cement. Even earlier, around 3000 BC, Egyptians made use of gypsum and lime mortars in their construction practices. The historical evolution of concrete includes various forms and nomenclatures across different civilization [27]; see Figure 1.

In the early 20th century, considerable efforts were dedicated to enhancing the compressive strength of concrete. The outcome of these efforts shows a substantial increase in concrete's compressive strength from 15 to 20 MPa until 1960. In 1970s, scientists and researchers had successfully achieved 60 MPa of concrete strength due to the availability of water reducer agents [11].

In 1981, with the invention of the High-Range Water Reducer (HRWR), also referred to as superplasticizer (SP), concrete technology entered an advanced phase of innovation [28]. At that time, researchers realized that the correct use of SP could reduce the water-to-binder ratio (W/B) to 0.30. Before the invention of SP, it was even beyond imaginable limits to reduce the W/C ratio to less than 0.30, until Bache [29] reported that using silica fume (SF) and a high percentage of SP, it was possible to achieve W/B of 0.16 [11].

Before the 1980s, producing UHPC was only possible in a controlled atmosphere, typically in laboratory settings, because of particular mixing and curing methods. Through the use of vacuum mixing techniques and heat curing procedures, researchers aimed to create a denser and more compact concrete mixture. These methods were employed to achieve an impressive compressive strength of up to 510 MPa [11,30].
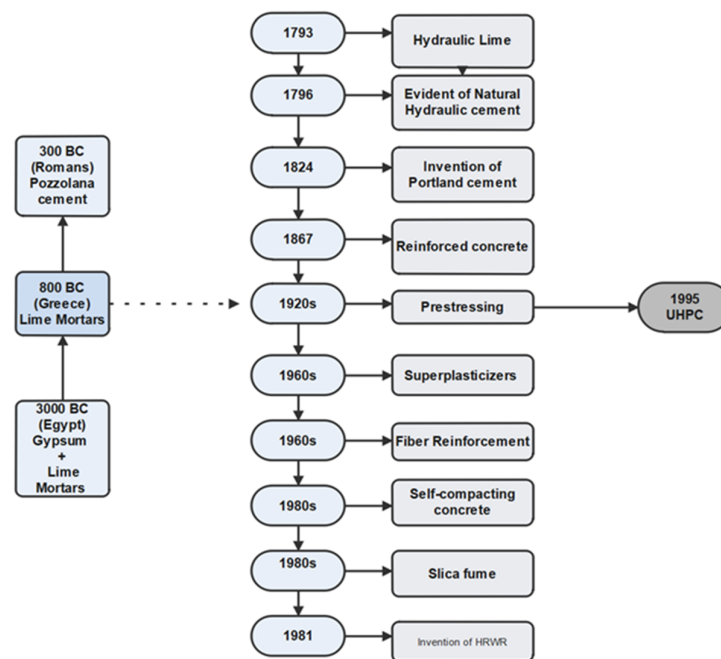
Figure 1. A brief overview of UHPC historical development.

By compacting granular materials and adjusting grain size distribution, a compressive strength of 280 MPa was achieved. This breakthrough indicated that low-porous materials had a tendency to develop ultra-high-performance Portland cement-based materials [9–11].

In the early 1980s, polymers were introduced to enhance the pore structure, aiming to eliminate defects in the cement paste. This innovation eventually led to the development of micro defect-free cement (MDF) [11,31]. A complicated procedure was required to produce MDF concrete for achieving compressive strength of 200 MPa. Complex production technique, expansive raw material, brittleness and creep had confined its applications [11,31].

Bache [27] in Denmark developed dense silica particle cement (DSP). In contrast to the production process of MDF, the production of DSP did not involve critical steps. Instead, the particle packing density was improved using a high dose of superplasticizer (SP) and SF to overcome defects in DSP. However, heat and pressure curing were also part of the production of DSP. Despite having a compressive strength of 345 MPa, DSP concrete exhibited increased brittleness [11].

Brittleness was the major problem that needs to be addressed, therefore in 80s steel fibres were introduced to overcome the brittleness issue of DSP concretes. The introduction of steel fibres into the concrete marked a significant advancement in concrete technology. This new material featured a dense microstructure, high compressive strength, superior durability and ductility. Following DSP, the invention of compact reinforced composites (CRC) and slurry infiltrated fibre concrete (SIFCON) were considered even better creations with superior mechanical properties and durability. However, both CRC and SIFCON faced workability issues due to the non-availability of efficient superplasticizers, which posed obstacles in on-site applications [11,31,32].

The invention of reactive powder concrete (RPC) is considered a significant breakthrough in the development of UHPC. RPC was invented by Richard et al. [15] in the 1990s, who employed thermal treatment to enhance the fineness and reactivity of the components used in RPC. The utilization of a very high cement content, SF, fine quartz powder and quartz sand with optimum gradation, along with the induction of SP and steel fibres, all contributed to the production of a highly approachable UHPC. This mixture, characterized by a very low water-to-cement (W/C) ratio, was suitable for both laboratory and field applications. To enhance homogeneity, coarse aggregates were intentionally omitted. Reactive powder concrete (RPC) demonstrated compressive strengths ranging from 200 MPa to 800 MPa, coupled with excellent workability features [10,30,33]. In 1997, the first-ever

structure made entirely of Reactive Powder Concrete (RPC) was constructed in Sherbrooke, Canada, and it was a pedestrian bridge [9,11,34–36]. The successful application of RPC was hindered by the unavailability for common usage due to expensive material and production costs.

From the year 2000 onward, researchers have shifted their focus to the development of inexpensive and eco-friendly UHPC. Rather than solely pursuing higher strength, there has been an emphasis on minimizing carbon dioxide (CO_2) emissions by reducing cement contents [25].

Until now, various methods and procedures have been explored to reduce cement content to less than 850 kg/m^3 and silica fume content to less than 200 kg/m^3. This reduction is achieved by incorporating supplementary cementitious materials (SCMs) and fillers into the concrete mixture [25,35,37–39], like fly ash, ground granulated blast furnace slag (GGBFS), rice husk ash and Metakaolin [10,11]. Also, researchers have tried to use standard curing methods instead of heat curing for energy saving [25,40,41].

In this new era, researchers are concentrating on creating UHPC using new materials and advanced technologies to address coupled issues and to expand the application of this state-of-the-art cementitious material. The goal is to maintain superior mechanical properties and durability [25].

2. Manufacturing and Design of UHPC

2.1. Composition of UHPC

Attaining excellent compressive strength and durability of UHPC, philosophy governed around four-points ideology [9], as noted hereunder:

1. **Low Water-Cement Ratio**. Maintaining a very low water-cement ratio, typically between 0.20 to 0.25, is crucial. This helps in achieving a compact and robust structure through hydration. The low ratio reduces capillary pores, enhances ductility and prevents brittle collapse.

2. **High Particle Packing Density**. Utilizing fine binder materials promotes high particle packing density, minimizing water demand in the fresh mixture. This not only improves compressive strength but also influences the brittleness of the concrete.

3. **Optimal Superplasticizer Dosage**. Employing a high dose of superplasticizer is essential for regulating the workability of UHPC. This ensures that the concrete is sufficiently workable while maintaining the desired properties.

4. **Use of Fibres**. Incorporating fibres serves the purpose of inducing tension and bending tension in the UHPC. This, in turn, increases shear strength and imparts the necessary ductility to the concrete.

However, unlike conventional concrete, where coarse aggregates are an essential part, the concept of using coarse aggregates is disregarded in UHPC for the purpose of increasing the homogeneity of the mixture [11,30].

Therefore, we can categorize the typical ingredients in new development of UHPC as:

- Binder materials;
- Aggregates;
- Fibres;
- Chemical admixtures.

2.1.1. Binder Materials

Typically, from 800 to 1000 kg/m^3 of binder material is used in the production of UHPC [7,10,30]. In the hydration process, 30–40% of the cement content contributes due to the very low water-to-binder (W/B) ratio in UHPC. Therefore, the remaining cement particles act as inactive filler [7,42]. It is noted that a UHPC mixture with a binder content of 500 kg/m^3 exhibits a significantly lower slump value. In contrast, a UHPC design mix with 700 kg/m^3 of binder content can achieve a flowability of up to 130 mm [7,43]. On the other hand, if the cement content in the UHPC mix design is replaced by 50–73%, the

compressive strength may drop by 100 MPa or even lower. This 50–73% replacement of cement contents in the mixture corresponds to only 280 kg/m^3 [7,44]. Therefore, there arose a necessity to introduce supplementary cementitious materials to decrease cement contents, subsequently reducing carbon emissions and enhancing flowability without compromising the mechanical properties of UHPC [7,45–48].

The most commonly used supplementary cementitious materials (SCMs) are such as fly ash (FA), ground granulated blast-furnace slag (GGBS) [49], silica fume, metakaolin [50], limestone powder [43], steel slag powder [51] and rice husk ash [52].

Portland Cement

Depending on the environmental conditions and the specific applications, UHPC can be produced with different types of cement, including Type I–V and white cement. However, Type III and white cement are the most commonly used cements as they shorten the setting time of concrete and enhance strength due to their high C3S content and Blaine fineness. On the other hand, Type I cement can be considered due to its lower cost and reactivity, especially when exceptionally high early stage strength is not a mandatory criterion [11,25].

Silica Fume

Silica fume (SF) is usually added to the mixture in quantities between 5% and 25%. In quantities below 10%, it improves the concrete particle packing density and workability due to its fine particle size. However, if the SF content exceeds 10% of the UHPC, it can substantially diminish workability, as the large surface area of the SF tends to absorb free water [53]. Moreover, owing to its high SiO$_2$ content, SF imparts a seeding effect and pozzolanic effect, enhancing cement hydration and refining the microstructure of UHPC [25].

Rice Husk

Rice husk is an agricultural waste which is used to replace SF, partially or completely, because of the amount of amorphous silica. The D$_{50}$ of rice husk ash is 50–100-times larger than SF, ranging from 5 μm to 20 μm. However, the surface area of rice husk ash is larger (i.e., 64,700 m^2/kg) than SF (i.e., 18,500 m^2/kg), thus increasing the water absorption and reducing the concrete workability [25]. Moreover, the rice husk ash absorbs water during the mixing process and gradually releases it during the hydration process, delays the internal dehydration and hence mitigates the autogenous shrinkage [10,25].

Fly Ash

Fly ash, a byproduct obtained from coal power stations [10], is primarily used in the production of UHPC with main emphasis on type C and type F fly ash. Both hydraulic and pozzolanic reactions are experienced in type C fly ash, whereas type F only undergoes pozzolanic reactions due to its lack of CaO. Fly ash is employed to replace cement, typically with ratios ranging from 40% to 60% for type C and from 10% to 30% for type F. The more spherical shape of fly ash compared to cement mitigates inter-particle friction, consequently enhancing the workability of the concrete [25,54].

Granulated Blast Furnace Slag (GGBFS)

Ground Granulated Blast Furnace Slag (GGBFS) has been employed as a supplementary cementitious material in concrete for an extended period [55]. The slag used in UHPC mixes can include copper slag, iron slag and barium slag. As an alternative SCM, slag typically replaces cement with ratios ranging from 30% to 60%. The angular shapes of slag particles elevate inter-particle friction, leading to decreased workability of UHPC in comparison to an equivalent quantity of fly ash [25].

Glass Powder

Glass powder is utilised as a substitute for cement or SF in UHPC mixtures with ratio from 10% to 50%. D_{50} of the glass powder ranges from 1 μm to 20 μm with a smooth surface which mitigates the inter-particle friction, water absorption and, thus, increases the workability of the concrete [56,57].

Metakaolin

Metakaolin, derived from the calcination of natural clay, is employed to enhance the early strength and durability of concrete. Concurrently, the incorporation of metakaolin powder can ameliorate autogenous shrinkage and refine the pore structure [10,58]. The use of metakaolin as a substitute for SF in the production of UHPC has been observed. It is noted that a high dose of metakaolin in UHPC may result in a reduction in compressive strength. Specifically, flexural strength increases by 2.6%, while compressive strength decreases by 6.7%. The availability, economical pricing and its white colour make metakaolin a preferred choice for UHPC production [10,58].

2.1.2. Aggregates

High-quality crushed quartz sand, typically with sizes ranging from 150 μm to 600 μm, is commonly used as an aggregate in the production of UHPC. However, the fine quartz sand can be substituted with alternative aggregates due to its high cost [25].

River sand can be used as an alternative to quartz sand [37,39]. Nevertheless, the particles in river sand are 5–8-times larger than those in quartz sand, with sizes ranging from 0 mm to 4.75 mm. The use of river sand can downgrade the particle packing density compared to fine quartz sand. Therefore, masonry sand, with a size range of 0–2 mm, is employed to enhance particle packing [39]. Masonry sand is generated by crushing coarse aggregates, leading to a particle shape that is more angular. This angular characteristic has the potential to negatively impact the workability of UHPC.

Limestone sand is characterized by its affordability, uniform composition, plentiful reserves and global accessibility [59–61]. Additionally, it is considered as a more suitable replacement for fine quartz sand in the production of UHPC. Reports indicate that the cost per unit of volume can be reduced by less than 40% [62].

The inclusion of coarse aggregates (size > 4.75 mm) is typically avoided in UHPC mixes. This is attributed to several drawbacks:

- The shape and angularity of coarse aggregates reduce the packing density of the concrete.
- The concentration of stress at the contact points between aggregates has the potential to create vulnerabilities in the concrete matrix.
- The interfacial transition zone (ITZ) between coarse aggregates and the UHPC matrix is weaker compared to the ITZ between sand and the UHPC matrix [25].

2.1.3. Fibres

Fibres are incorporated into UHPC to improve tensile properties by impeding the initiation and propagation of cracks. The attributes of fibres, such as their material (texture), aspect ratio, shape and surface conditions, play a significant role in influencing the properties of UHPC [25,63–65].

Steel, carbon, wollastonite, basalt, polyvinyl alcohol (PVA), polypropylene-polyethylene (PP-PE) and biochip are types of hybrid fibres with different sizes [7,66] and shapes [7]. Among the various types of fibres, steel fibres stand out as the most frequently employed in UHPC. It has been observed that as the steel fibre content increases from 0% to 2% (by mass of the mixture), it significantly affects the 28-day flexural strength and toughness of UHPC [67–69]. On the other hand, the addition of steel fibres from 0.5% to 2.5% in the UHPC mix abruptly reduces the slump value from 4.29 to 1.10 [70].

2.1.4. Chemical Admixtures

Chemical admixtures are utilised to alter the fresh and/or hardened properties of UHPC. Specifically, high-range water reducer (HRWR) is employed to attain self-consolidating properties. Among various types of HRWR, polycarboxylate ethers (PCE) exhibit high efficiency in dispersing cement particles [71]. Nevertheless, the absorbed high-range water reducer (HRWR) on cementitious particles can disrupt the hydration reaction, leading to an extension of the setting time and a reduction in mechanical strength during the early stages [25].

2.2. Design Methodology

As mentioned earlier, high particle packing density, low void ratio and high mechanical properties form the basis for designing UHPC mixtures. Consequently, three models have been introduced based on the above concept: the dry particle packing method, wet particle packing method and performance-based method [25].

2.2.1. Dry Particle Packing Method

The dry particle packing model presented by Anderson and Andreasen to achieve the maximum packing density of UHPC mixtures is widely adopted [70]. However, this model considers particles under dry conditions only. Dry particle packing method is further divided into two models: the discrete model [72–75] and the continuous model [76].

The first continuous model, developed by Fuller and Andersen by introducing the target particle size distribution $P(D)$, is considered the most preferred choice for the design of UHPC mixtures [25,76]. The modified Andreasen and Andersen model was introduced by Funk and Dinger [64], taking into consideration the minimum particle size effects on particle packing. $P(D)$ is calculated as follows, see Equation (1).

$$P(D) = \left(\frac{D^q - D_{min}^q}{D_{max}^q - D_{min}^q} \right) \cdot 100\% \tag{1}$$

In the above equation, D is the target particle size (μm), D_{min} represents the minimum particle size (μm) in all materials and D_{max} represents the maximum particle size (μm). The distribution modulus, q, is a parameter, and for fine particles, a q value of 0.23 ($q < 0.25$) is recommended [11,77].

The disadvantage of the dry particle packing methods is that they only consider particles under dry conditions, which may not accurately reflect the real/actual particle packing of UHPC mixtures due to the presence of water and other chemicals [78].

2.2.2. Wet Particle Packing Method

The wet particle packing model considers the effect of water and HRWR. The following steps must be considered to obtain the wet particle packing density [78]:

- Assume the initial W/B.
- Weigh the water and binder materials and mix them.
- Pour the paste into a cylindrical mould and weigh.
- Calculate the solid concentration (Φ) and void ratio (u) form the Equations (2)–(4).
- Achieve the maximum packing density by repetitions of above steps.

$$V_S = \frac{M}{\rho_w \mu_w + \rho_\alpha R_\alpha + \rho_\beta R_\beta + \rho_\gamma R_\gamma} \tag{2}$$

$$u = (V - V_S)/V_S \tag{3}$$

$$\varnothing = V_S/V \tag{4}$$

In Equation (2), V_S is a solid volume of the particles; M and V refer to the mass and volume of the mixture in the mould, respectively; ρ_w refers to the density of water;

μ_w refers to the volumetric ratio of water; ρ_α, ρ_β, and ρ_γ refer to the solid density of different binder materials, respectively; and R_α, R_β, and R_γ refer to the volumetric ratios of binder materials, respectively.

In Equation (3), u refers to the minimum void ratio, and in Equation (4), Φ represents the maximum solid concentration. However, the expected results are not achieved by solely optimizing the maximum particle packing density of UHPC [25].

2.2.3. Performance Based Method

A performance-based method was developed by Meng et al. [39] to enhance the non-proprietary UHPC [25]. The step-by-step procedure is illustrated below, and the process is also demonstrated in the flow chart in Figure 2:

- Select binder materials based on the flow properties of the paste.
- Consider material combinations in terms of particle packing, flowability and mechanical properties.
- Evaluate rheological properties, such as plastic viscosity (μ_p) and yield stress (τ_0), to confirm the composition of the mix.
- Determine the workability and compressive strength as key properties to determine the w/b ratio for the mix.
- Use the modified Andreasen and Andersen model to determine the sand gradation, calculate the ratio between the volume of the primary paste and the sand volume of the mortar, and compute the steel fibre content.
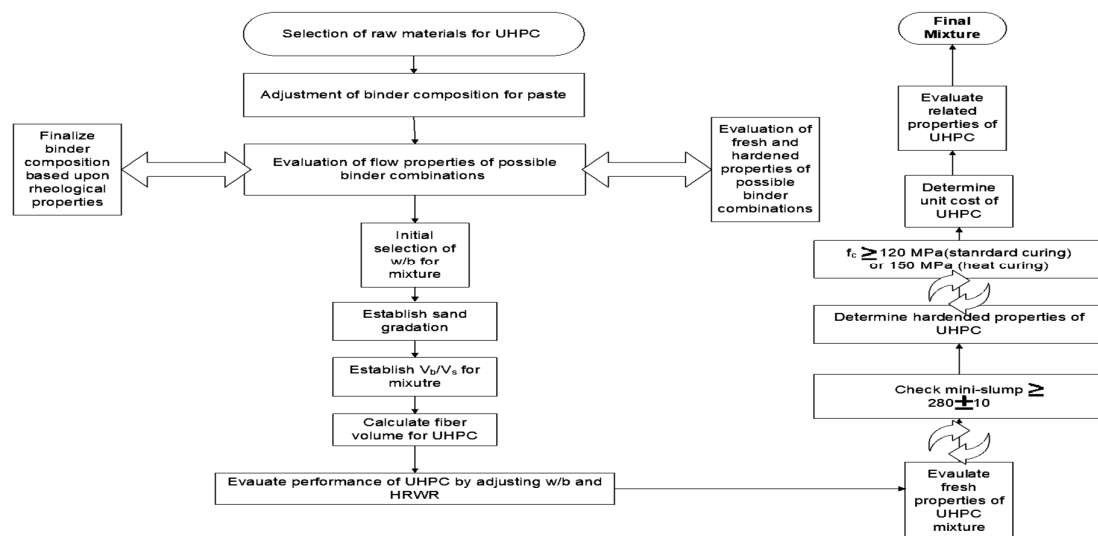- Finalize making UHPC concrete mix as per the given instructions.

Figure 2. Flow chart of a performance-based method [39].

3. Production

Nowadays, the UHPC mixture is mixed, cast and vibrated like conventional concrete. The production procedural steps are as follows [10,18]:

- Mixing of all dry materials for about 10 min.
- Add water and superplasticizer into dry mixture and mix for approximately 5–10 min.
- Fibres are added if required.
- Finish the mixing when mixture shows enough flowability for good workability and sufficient viscosity.

The mixing procedure for UHPC appears to take a longer time than that for conventional concrete and consumes more energy. Due to the absence of coarse aggregates and the low W/B ratio, a specific sequence needs to be followed to prevent the UHPC mixture from overheating [79]. Table 2 represents the different compositions of UHPC mixtures,

including the quantity of cement utilised in producing one cubic meter of UHPC, along with the fibre type and percentage.

Table 2. Typical composition of UHPC.

Composition	Sequence	Type of Fibre	Length and Diameter	Amount of Fibres Vol. % or kg/m³	Cement kg/m³	Ref.
PC + SF + Q		Steel Fibre	13 mm × 0.16 mm ∅	2–2.5	788	[16]
			6 mm × 0.16 mm ∅			
PC + FA + SF		Steel Fibre	13 mm × 0.20 mm ∅	1–3	642–662	[80]
PC + FS+ SF		Steel Fibre		0–2	712	[16]
PC + SF + FA		Steel Fibre	20 mm × 0.20 mm ∅	1	360–900	[16]
			25 mm × 0.30 mm ∅			
PC + FA + GGBS		Steel Fibre		0	582.1–896.3	[81]
PC + SF + QP		Glass Fibre	6 mm × 0.015 mm ∅	12 *	750	[82]
PC + SF + UFSP		Polypropylene	12 mm × 0.050 mm ∅	0–78	737–1005	[83]
PC + MK + NMK					720–800	[16]
PC + MK+ FA					482	[84]
PC + MK + LS					608	[84]
PC + GGBS + QP + FS	GGBS 30%	Steel Fibre	13 mm × 0.20 mm ∅	2	630	[85]
PC + GGBS + QP + FS	GGBS 40%	Steel Fibre		2	540	[85]
PC + GGBS + QP + FS	GGBS 50%	Steel Fibre		2	450	[85]
PC + FA + QP + SF	FA 20%	Steel Fibre		2	720	[85]
PC + FA + QP + SF	FA 25%	Steel Fibre		2	675	[85]
PC + FA + QP + SF	FA 50%	Steel Fibre		2	630	[85]
PC + MK + SF	MK 15%	Steel Fibre		2	765	[85]
PC + MK + SF	MK 20%	Steel Fibre		2	720	[85]
PC + MK + SF	MK 25%	Steel Fibre		2	675	[85]
PC + SF		Metal fibre	13 mm × 160 μm ∅	138 *	691	[86]
PC + MK		Metal fibre		138 *	691	[86]
PC + FA + SF		Straight steel fibre	13 mm × 0.20 mm ∅	156 *	754	[87]
PC + FA + SF + MK				156 *	754	[87]
PC + FA + MK				156 *	754	[87]
PC + SF + QS		Basalt Fibre	12 mm × 15 μm ∅	0, 0.5, 1.0, 2.5	706	[88]
PC + SF + QP + QS		Basalt Fibre	12 mm × 18 μm ∅	6 *	876	[89]
PC + GP + SF + WG		Basalt Fibre	24 mm × 16 + 0.2 μm ∅	8.1 *	720–400	[90]

PC is Portland cement, SF is silica fume, Q is quartz, FA is fly ash, FS is fine sand, GGBS is granulated blast furnace slag, QP is quartz powder, UFSP is ultra-fine silica powder, MK is Metakaolin, NMK is nano metakaolin, LS is limestone, GP is Geranium plant, WG is waste glass; * referred to the density of fibres.

3.1. Sampling

The preparation of UHPC samples for testing purposes is no different from that for conventional concrete. Both cubes and cylinders can be used for sampling or to perform compression tests. Nevertheless, advanced studies have shown that cubes are more suitable for compression tests than cylinders (Figure 3).

Figure 3. Typical UHPC samples, (**a**) made of cubes and (**b**) reinforced with fibres.

3.2. Curing

A suitable curing process is crucial for optimizing the performance of any concrete. UHPC requires less additional curing compared to other concretes because it is designed based on rheological behaviours and optimised gradation of granular materials. However, UHPCs still require proper hydration [79]. Design mix ratios of each material and curing techniques affect the properties of UHPC [91–93].

Since the design of UHPC is based on a very low W/B ratio, a more precise curing method is essential to prevent water outflow before the hydration process. Therefore, the freshly cast exposed surface of UHPC needs to be carefully packed immediately to prevent surface dehydration. Materials such as metal, plastic or wood sheets are considered most suitable for packing the UHPC surface [79].

Below methods are most commonly used for curing:

- Standard room temperature curing;
- heat curing under atmospheric pressure;
- autoclave curing;
- fog;
- steam.

The most economical and eco-friendly method is a standard room temperature curing. However, better compressive strength results can be achieved with a 24 h steam curing method than with a 28-day standard room temperature method [10,94]. It was also found that the compressive strength of UHPC was higher when cured in an autoclave for 8 h compared to standard curing at room temperature and heat curing [95]. The effects of different curing methos on the compressive strength, [37,43,48,49,52,55,86,96–117], are shown in Figure 4.
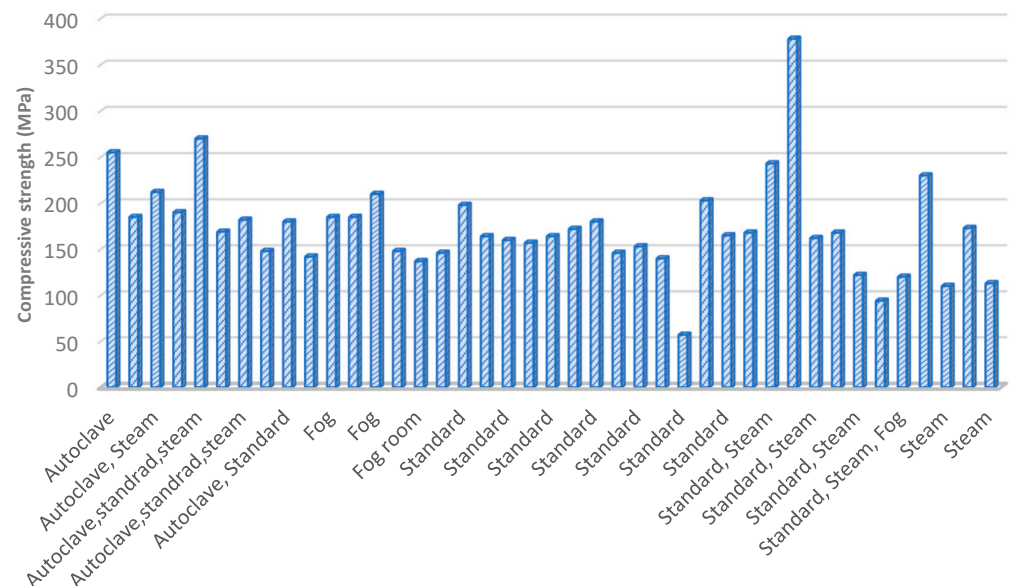

Figure 4. Effects of curing methods on compressive strength.

4. Mechanical Properties of UHPC

UHPC has already demonstrated excellent mechanical properties. However, the mechanical properties of UHPC are still heavily influenced by the material's composition, mix proportions and the applied curing methods [118]. In the following subsections, various mechanical properties of UHPC are explained in the above context.

4.1. Compressive Strength

Compressive strength is a key property of any concrete. Standard testing methods for compressive strength, such as ASTM C39 and ASTM C109, are also applicable to UHPC [79,119,120].

Researchers have found that a compressive strength of 200 MPa may be achieved in a UHPC mixture by replacing 30–35% of cement with SF [10,121].

The authors of [58] found that UHPC with metakaolin had the same or slightly lower compressive strength than UHPC with SF. It is also noted that applying heat curing to UHPC, incorporating metakaolin along with either crushed quartz or steel fibres, leads to a

further increase in compressive strength. In another study, the researchers found that the maximum compressive strength is achieved when Mmetakaolinmetakaolin replaces 15% of the cement [84].

In a recent study by Chen et al. [122], a binder material incorporating SF with a particle size ranging from 8 to 13 μm was utilised, complemented by fine aggregate sourced from quartz particles with a size from 0.15 to 0.84 mm. To further augment the bulk density of the mixture, a special type of quartz powder with an average particle size of 15 μm was incorporated. Polycarboxylate-based superplasticizer (SP) was also utilised. The study incorporated micro basalt fibre, macro basalt fibre and steel fibre both individually and in various combinations in the UHPC mixture. The results showed that the compressive strength of the UHPC mixture without any fibre and with micro and macro basalt fibres was almost the same, measuring 127.6 MPa and 128.5 MPa, respectively. However, the mixture containing only macro basalt and only steel fibres (3% by volume) exhibited compressive strengths that were 17.6% and 28.6% higher than the mixture without any fibre.

Moreover, it has been documented that surpassing a 2% fibre content in the UHPC mixture does not result in a substantial effect on compressive strength [123]. The evolution of UHPC strength trends, as documented in previous studies [37,43,48,49,52,55,85,87–90,96–98,100–116], is shown in Figure 5.
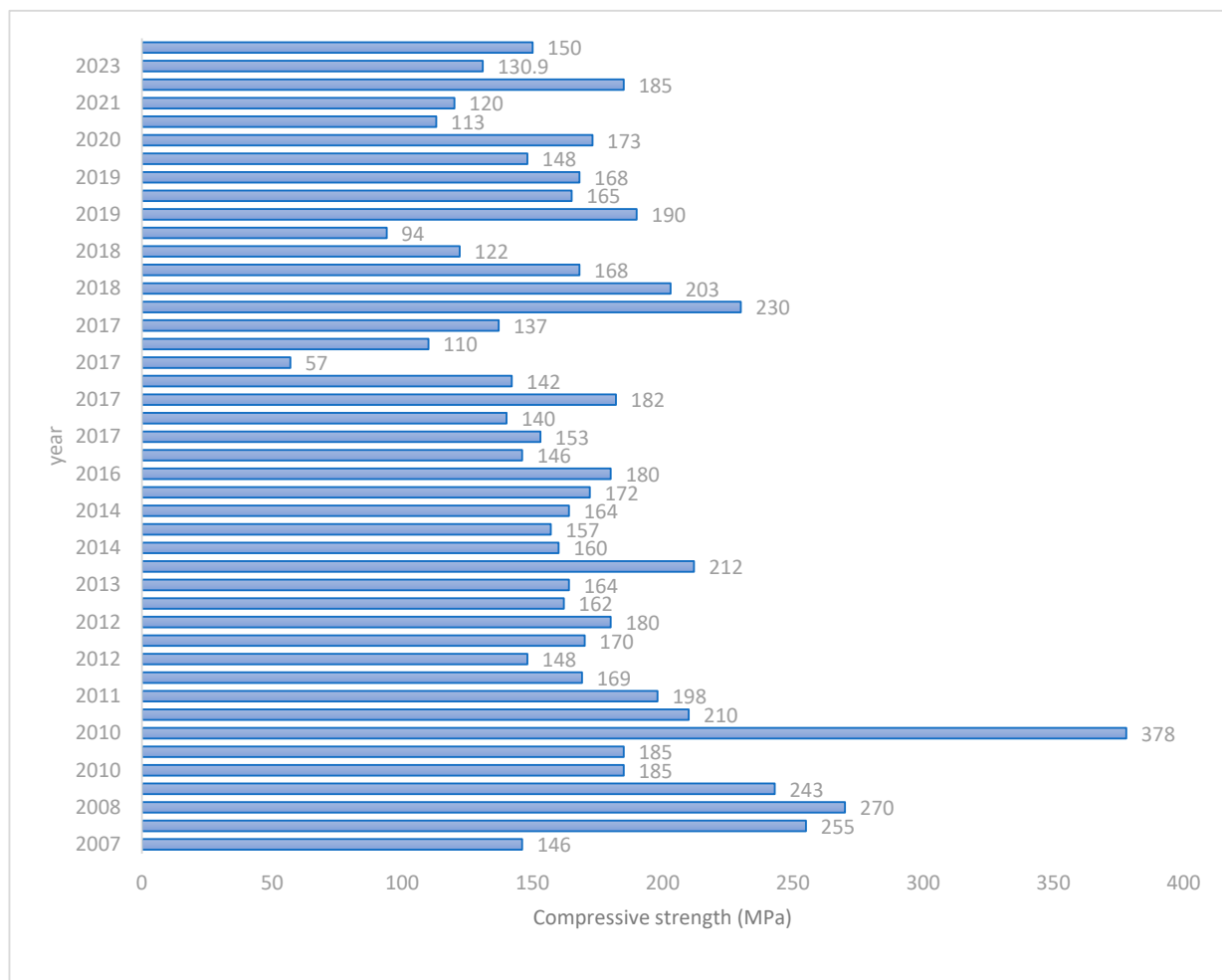

Figure 5. An overview of the UHPC strength trends.

4.2. Flexural Strength

The researchers revealed that a UHPC mix containing SF or metakaolin had almost the same flexural strength regardless of the presence or absence of fibres and regardless of the curing method. However, the use of fibres in the mixture may enhance flexural

strength, especially when the mixture includes fibre contents and undergoes heat treatment. In contrast, mixtures without fibres and without heat treatment exhibit higher flexural strength [58]. However, the maximum flexural strength is achieved by substituting 15% of metakaolin [16].

A brittle behaviour is observed in UHPC when it does not contain any fibre content. However, the addition of macro basalt fibres or steel fibres (3% by volume) to the mix results in UHPCs with higher flexural strengths of 28.5 MPa and 31.8 MPa, respectively [122].

The integration of steel fibres in UHPC plays an important role in achieving structural reliability through load transfer phenomena across cracks, increasing flexural strength in UHPC mixtures [124]. The literature has also shown that increasing the fibre content in the UHPC mixture does not really improve the flexural strength [124].

5. Recent Innovations and Research in UHPC

The development of UHPC is progressing daily, consolidating its status as one of the most exceptional concrete materials currently available, characterized by its well-known properties; see Table 3.

Table 3. Properties of ordinary concrete (OC), high-performance concrete (HPC) and UHPC.

Property	Ordinary Concrete (OC) [27]	High-Performance Concrete (HPC) [125]	Ultra-High-Performance Concrete (UHPC) [126]
Compressive Strength (MPa)	<50	60–100	>120
Flexural Strength (MPa)	<5.4	8.94	>12
Cement (kg/m^3)	<400	425–500	746
Water-Cement Ratio	>0.35	0.4	0.24
Coarse and Fine Aggregates Ratio	1:0.70	1:0.54	0:1
Admixtures Used	-	Superplasticizer	Superplasticizer
Curing Method	28 days water curing	28 days water curing	28 days water curing
Special Ingredients	-	Metakaolin and steel fibres	Metakaolin/Micro Silica and basalt fibres
Application/Use Cases	Construction and Infrastructures	Construction and Infrastructures	Construction, Infrastructures, high elevated temperature zone, harsh marine environment and high security zone construction

UHPC is recognized for its remarkable strength and durability, coupled with a notably low porosity, high packing density and minimal permeability [64,127]. To achieve UHPC with exceptional strength, durability and increased sustainability, several considerations come into play. These strategies involve the exclusion of coarse aggregates exceeding 5 mm, the reduction of W/C ratio facilitated by superplasticizers, and the substitution of Ordinary Portland Cement with various SCMs such as GGBS, fly ash, metakaolin and rice husk ash [52,117,128,129].

Research findings indicate that Ultra-High-Performance Fibre-Reinforced Concrete (UHPFRC) possesses remarkable tensile and flexural strengths compared to ordinary concrete. The addition of steel fibres plays a crucial role in enhancing the mixture's mechanical properties. Specifically, the incorporation of 2% volume of steel fibres results in a significant increase of up to 228% in tensile splitting strength and 180% in flexural strength.

The use of long fibres further elevates the load-carrying capacity and strain hardening performance of UHPFRC. Notably, UHPFRC exhibits outstanding energy absorption and dissipation capabilities, surpassing those of ordinary concrete. In addition, its resistance to crack formation and transmission makes it a more favourable building material [13]. The introduction of steel fibres changes the failure pattern of UHPFRC from brittle to ductile failure [130]. While there is no doubt that steel fibres play an important role in enhancing the tensile strength of UHPC, their influence on the compressive strength appears to be uncertain. Other factors, such as variations in test specimen geometry and additional parameters, could also contribute to influence the results [26].

Despite the acknowledged environmental advantages of incorporating SCMs such as fly ash, rice husk ash and GGBS as replacements for cement in UHPC, many researchers believe that the diverse chemical compositions pose a challenge, leading to unreliable performance [131]. The purity and efficiency of raw materials in production plants is directly proportional to the chemical compositions [132]. As a consequence, the commercial application of UHPCs with SCMs as cement replacements still remains quite limited [25].

UHPC encounters challenges in establishing widespread usage. While it demonstrates success on a laboratory scale, difficulties arise when attempting large-scale operations, potentially leading to mixer failures [133]. The volume production of batches is consequently limited. Another important factor standing in the way of wider acceptance is the high cost associated with the components used in UHPC, particularly the expensive cement, silica fume and steel fibres. For instance, a typical strain-hardening UHPC [134,135] comprises 1100–1300 kg/m^3 of cement and 200–350 kg/m^3 of silica fume, constituting 18–26% of the mass of the binder material [115]. Table 4 reflects the difference between mechanical properties and effect of different methods of UHPC with SF and with metakaolin.

Table 4. Comparison between the properties of UHPC with silica and UHPC with metakaolin [58].

W/B	Silica Fume %	Metakaolin %	Steel Fibre kg/m³	Curing Methods		Compressive Strength	Flexural Strength
				Method	Hours/Days	MPa	MPa
0.22		25		T @ 90 °C	70/5	133	5
				T @ 150 °C	70/5	141	11
	25		164	T @ 90 °C	70/5	126	6
				T @ 150 °C	70/5	140	14
		25	165	T @ 90 °C	70/5	204	34
				T @ 150 °C	70/5	234	34

The findings indicate that metakaolin exhibits a higher level of reactivity compared to SF and demonstrates comparable or superior effects in enhancing both mechanical properties and durability. Several studies have dealt with the incorporation of metakaolin in UHPC [9,86]. UHPC with metakaolin exhibited almost equivalent mechanical properties, albeit with a slightly longer mixing time, and was considered as a substitute for SF. Notably, metakaolin contributed to a 13% increase in flexural strength [58,136].

A wet packing method considers the water absorption of metakaolin, to elevate the mass ratio of metakaolin to cement. Subsequently, engineers designed a mixture of UHPC where metakaolin was completely replaced by SF and observed that no significant changes in mechanical properties occurred [115]. Metakaolin was swapped with two-thirds of SF in a UHPC design mix. Advanced autogenous shrinkage was noticed with respect to the reference mix design, which was purely based on SF [115]. Furthermore, the addition of metakaolin in the UHPC mix significantly reduced the drying shrinkage in contrast to UHPC with only SF [99]. Metakaolin in UHPC also exhibited better permeability resistance [86].

Basalt fibres are considered superior due to their equivalent mechanical strength, their enhanced durability compared to glass fibres, their lower cost compared to carbon fibres, their sustainability resulting from abundant raw materials and their environmentally friendly production process [137]. The outstanding mechanical properties of basalt, particularly within broad temperature ranges, contribute to the preservation of concrete integrity [89].

The thermally treated sugar cane bagasse ash (SCBA) exhibited measured compressive, tensile and flexural strengths at 162.5 MPa, 17.78 MPa and 24.05 MPa, respectively, after treatment at 700 °C [138]. Additionally, in Ultra-High-Performance Fibre-Reinforced Concrete (UHPBFC) mixes, a thermally treated rice husk ash was incorporated, replacing two-thirds of the cement by volume. This resulted in a significant improvement in strength performance, with a respective increase in compressive strength of 9.7%, 14.5% and 10.2% at 7, 28 and 120 days in the mixtures, respectively [38].

The performance of UHPC has undergone extensive investigation through the incorporation of various industrial and agricultural wastes. However, a notable gap exists in

research regarding the utilization of waste from the perfume or geranium industry in concrete. This gap is particularly significant in light of prevailing climate and environmental concerns related to CO_2 emissions. Exploring these specific waste materials in concrete can offer valuable insights into their potential impact on UHPBFC performance and contribute to sustainable and environmentally conscious concrete practices [90].

The impact of integrating basalt fibre into the concrete mixes was noticeable in terms of increased toughness and elongation of the time between the initial appearance of the first crack and the ultimate failure [139]. The addition of basalt fibre can significantly improve bonding properties [140].

Basalt fibre possesses the capability to shift the failure mode of Basalt Fibre-Reinforced Polymer Composites (BFRPC) from tensile failure to tensile shear failure. Additionally, it effectively increases the stress level during cracking, consequently minimizing damage in BFRPC [141]. This observation implies that UHPBFC demonstrates enhanced thermal resistance when subjected to elevated temperatures [142].

Recent global climate changes have led to a demand for materials that are able to meet the structural requirements imposed by these changes. UHPC has emerged as a material that can fulfil these demands. In contrast to conventional concrete, UHPC offers a unique combination of properties that make it particularly suitable for modern structures/buildings that have to withstand extreme weather conditions. In addition to its fundamental superior mechanical and durability properties, UHPC has the potential to act as a smart and multifunctional concrete. Such smart and multifunctional building materials can exhibit additional properties, such as superhydrophobicity, self-healing, self-sensing, self-cleaning, self-luminescence, high-water repellence and conductivity, which increase their overall benefits (Figure 6) [143].
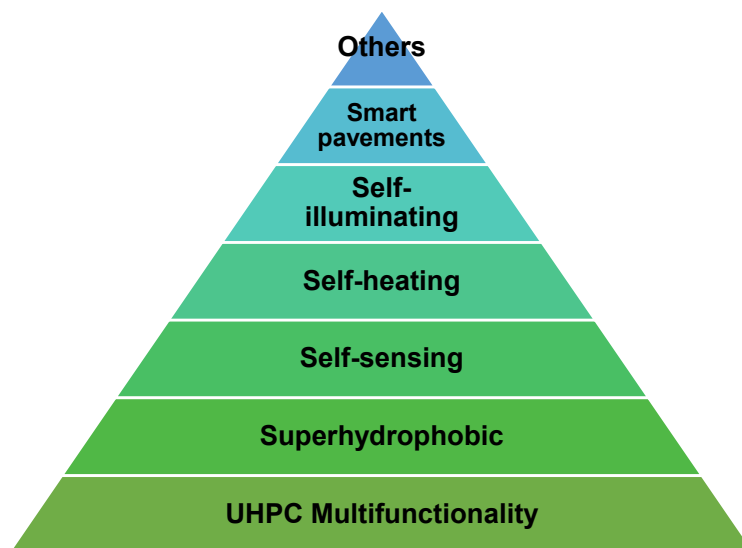

Figure 6. Suggested options for integrating UHPC with multifunctionalities such as superhydrophobic, self-sensing, self-heating, self-luminescence, etc.

5.1. Superhydrophobic Concrete

The natural hydrophilicity of concrete poses a potential risk to its mechanical durability, and it can contribute to structural failure. This vulnerability arises from the ease with which water can infiltrate the porous structure of concrete, leading to damage through freeze–thaw cycles, chemical erosion and other weathering factors. In response to this challenge, researchers have dedicated efforts to developing techniques aimed at improving the water-resistance of concrete [144–147]. Diminishing the water-to-cement ratio and incorporating extra cementitious materials to the concrete mix are widely regarded as common practices to mitigate the deterioration process of concrete structures [148–150].

In recent times, significant attention has been directed towards minimizing water infiltration and enhancing the durability of concrete [144,147]. Current strategies involve refining pore characteristics and increasing density by adjusting the water-to-cement ratio while incorporating supplementary cementitious materials [148,150].

The idea of superhydrophobic concrete has proven to be a promising strategy to enhance the resistance of concrete. According to the Laplace-Washburn equation [151], the capillary negative pressure plays a vital role, and elevating the water contact angle (WCA) can generate a more potent repellent force. This force actively expels water from pores, enhancing the concrete's water-resistant properties. Two primary techniques, surface and bulk modifications, are utilised to create superhydrophobic concrete.

Surface modification using hydrophobic agents has been practiced since 1986 [152]. For instance, in the Netherlands, the Ministry of Transport applied a hydrophobic coating to concrete bridges, resulting in an 80% decrease in chloride infiltration during de-icing salt cycles compared to the control sample [153].

Regarding bulk modification, the adding of a hydrophobic admixture effectively inhibited the corrosion of the reinforcement in concrete [154]. Moreover, the induction of bacterial biofilm during casting produced spike-like crystal structures, resulting in a hydrophobic hybrid mortar with exceptional resistance to various water sources [22].

Achieving superhydrophobicity usually involves applying hydrophobic substances on the concrete surface or within shallow surface pores, creating continuous protective coatings for enhanced long-term durability upon solidification. In contrast, bulk modification entails the direct mixing of hydrophobic modifiers with cement, which leads to their accumulation on the cementitious hydration products during the moulding process [22].

5.1.1. Surface Modification Method

Nanocomposite coatings, incorporating inorganic nanoparticles (NPs), typically outperform pure polymers due to improved mechanical stability, high temperature resistance and water-repellent properties. The sol-gel method, a straightforward approach, is used to create superhydrophobic nanocomposite coatings. SiO_2 NPs are commonly used in this method due to their chemical stability, straightforward synthesis and adjustable size. For example, Gao et al. [155] investigated the effectiveness of superhydrophobic asphalt concrete by blending hydrophobic fluoro silanes with SiO_2 NPs.

The 'mix + paint' technique has been employed, utilizing stable and functional polymers as adhesives to securely anchor particles. Typically, polydimethylsiloxane (PDMS) is used to create superhydrophobic surfaces due to its exceptional attributes, including chemical inertness, non-toxicity, cost-effectiveness, biocompatibility and eco-friendliness [127,156].

Despite established methods for producing superhydrophobic concrete materials, challenges persist in their practical application. These materials must maintain both structural integrity and durability, especially under prolonged UV exposure. Additionally, achieving superoleophobicity is crucial, as contaminated superhydrophobic surfaces lose their self-cleaning abilities with oil-based substances. It is noteworthy that SiO_2 nanoparticles might not meet these criteria, prompting exploration into alternative nanoparticles [22].

Achieving superhydrophobicity usually involves applying hydrophobic substances on the concrete surface or within shallow surface pores, creating continuous protective coatings for enhanced long-term durability upon solidification. In contrast, bulk modification involves directly mixing hydrophobic modifiers with cement and their accumulation on cementitious hydration products during moulding [22].

5.1.2. Bulk Modification Method

Silane and siloxane, known for their compact molecular structures, can permeate concrete's dense composition and chemically interact with the cementitious substrate. Both silane and siloxane, individually or combined, have demonstrated effectiveness in altering concrete [154,157]. For example, self-cleaning concrete is achieved by incorporating silane

into the mixture [158]. The introduction of low-surface-energy agents during moulding can yield superhydrophobic concrete. However, this approach alters the original structure, potentially impacting performance, leading to reduced compressive strength due to internal hydrophobization [22].

Siloxane-based admixtures, such as polyethylhydrosiloxane (PEHSO) and polymethylhydrosiloxane (PMHS), as mentioned in the literature [135], exhibit robust reactivity. These additives react with -OH groups of $Ca(OH)_2$, forming a durable hydrophobic cross-linked structure that bonds with cement hydration products via siloxane oligomers' polymerization.

In contrast to the surface modification, the bulk modification has a significantly effect on the concrete strength. Incorporating hydrophobic chemicals, including silane-based compounds and polydimethylsiloxane PDMS, typically results in substantial reductions in both compressive and flexural strength [121,159]. For instance, Song et al. [159] observed a 40.5% decrease in compressive strength and a 33.3% decrease in flexural strength with the addition of fluoroalkyl silane. Additionally, Subbiah et al. [83] noted a significant 60% decrease in compressive strength with fluoroalkyl silane and SiO_2/TiO_2 nanoparticles, rendering such concrete unsuitable for construction purposes.

In 2022, a green superhydrophobic hybridization model was introduced, integrating biomimetics (lotus effect), chemistry (siloxane and silane admixtures) and nanotechnology (SiO_2 nanoparticle hydrophobic coating) to create superhydrophobic concrete. This model demonstrated exceptional hydrophobicity, achieving contact angles (CA) of up to $157.6 \pm 3.1°$ and roll-off angles (RO) of $6.5 \pm 1.5°$, even when subjected to high-surface mechanical abrasion [160].

5.2. Self-Sensing UHPC

The concept of "smart concrete structures" was initially introduced by American researchers, particularly Chen P-W, in conjunction with the development of self-sensing concrete. Subsequent research and practical experiments have demonstrated that the combination of concrete and carbon fibres can serve as a strain or stress sensor [161].

The manufacturing process involved impregnating precast graphene nanoplate/cement-based sensors with silane/isopropanol solutions. The cement-based sensors treated with silane exhibited satisfactory performance in sensing stress and strain, boasting an average gauge factor of 141.8. Additionally, these sensors indicated outstanding hydrophobic properties, as evidenced by the greatest water contact angle of 163° on the intact surface [162].

The study investigated the mechanical, electrical and self-sensing characteristics of UHPC with stainless steel fibres and copper-coated steel fibres (CCSFs). The inclusion of 1.2 vol% CCSFs was found to significantly enhance the flexibility of UHPC, resulting in a 33.7% increase in peak compressive strain. UHPC reinforced with stainless steel fibres and CCSFs demonstrated excellent synchronization and repeatability of its self-sensing feature when subjected to three different cyclic loading amplitudes within the elastic range.

The strain sensitivity of UHPC reinforced with stainless steel fibres reached a maximum value of 26.6 under a cyclic compressive load of 37.5 MPa. In addition, UHPC with 1.2 volume percent of CCSFs achieved a strain sensitivity of 28.2 under a monotonic peak load, where the compressive stress was monitored in the range from 0 to 125.7 MPa. The electrical resistance of UHPC with stainless steel fibres/CCSFs can be used for the real-time monitoring of stress, strain and damage evolution in structures [12].

5.3. Self-Heating UHPC

The self-heating capability, active de-icing and snow-melting performances take the UHPC to the next level. Self-heating composites were produced and assessed. The UHPC slab, reinforced with stainless steel wires (SSWs), exhibited consistent electrical conductivity and robust self-heating capability throughout repeated cycles. Moreover, it demonstrated effective active de-icing and snow-melting properties under various environmental conditions [163].

5.4. Other Concepts

According to statistics, the electricity consumption of street lighting accounts for around 20–30% of the total electricity consumption of national lighting. Nevertheless, the power utilization rate is below 65%, which indicates a considerable waste of energy [164]. One possible solution to this problem is to provide road surfaces or associated concrete components with self-illuminating properties by integrating built-in illumination devices or luminescent materials. This approach not only has the potential to save energy and reduce environmental light pollution but also to solve problems such as uneven illumination and glare associated with conventional streetlights [165]. Developed countries, including Germany, the United States and France, have already begun researching and developing self-luminous pavements [166]. The integration of self-luminescent properties into concrete materials is a novel concept in civil engineering and has been the subject of recent research [131].

German artist Konrad Lueg introduced one of the first light-emitting projects by inducing phosphorescent paints as smart materials like the "Schattenwand mit Blitzelektronik" [167]. Some successful engineering applications of luminous pavements have been accomplished. In 2012, the Dutch studio Roosegaarde presented the idea of a luminous highway as part of a smart highway project [168]. Thus, UHPC, known for its excellent mechanical properties, durability and versatility, can serve as an ideal material for the integration of smart functions, including self-luminescence.

Intelligent manufacturing of UHPC, specifically through 3D printing, represents a recent and innovative approach that combines optimal design through computer-aided technology with the use of particle packing models and machine learning techniques. This approach aims to achieve high efficiency and accuracy in predicting the properties of the resulting UHPC [15].

5.5. Multifunctionality

Our latest experimental work has focused on the development of an innovative basalt-reinforced UHPC that offers multifunctionality through the simultaneous integration of self-cleaning and self-illuminating properties. The produced samples, characterized by high particle packing density, show adequate workability and achieve high compressive strength. The incorporation of basalt fibres significantly reduces brittleness. To ensure the desired long-lasting visual appearance of decorative UHPC and minimize future maintenance costs, we introduced a time-effective strategy to create a light-emitting biomimetic surface design [126].

The prospects for UHPC, enhanced with superhydrophobic and self-luminescent features, represent a transformative path for civil engineering and infrastructure development. Incorporating superhydrophobic properties not only increases durability but also reduces maintenance costs and improves resistance to environmental pollutants. At the same time, the integration of self-luminescent properties creates a breakthrough solution for efficient lighting at night, demonstrating the potential for a concept shift in construction technology.

6. Durability of UHPC

UHPC is a material designed to withstand harsh environmental conditions. Consequently, the assessment of its durability is considered essential. The evaluation of UHPC durability primarily focuses on water and chloride-ion permeability, corrosion of steel reinforcement, freeze–thaw resistance and fire resistance [150]. A brief assessment of the durability of UHPC is therefore provided below.

6.1. Water Permeability

In the previous section, it was discussed that the hydrophilic nature of concrete can adversely affect its mechanical durability and potentially lead to failures due to the corrosion of steel rebars and/or fibres [150]. However, UHPC exhibits lower porosity and a denser microstructure, providing assurances of excellent permeability resistance [36,169]. UHPC

is designed at a low W/B and low porosity, which is the origin of its high permeability resistance quality [148,170].

6.2. Chloride-Ion Permeability

Two testing methods are defined to assess chloride-ion permeability. One is the Rapid Chloride Permeability Test (RCPT), and the other is the Nordtest method NT Build 443 [150]. In the Nordtest method, NT Build 443 coefficient of chloride ion diffusion is the main determining factor to evaluate the chloride-ion permeability; for UHPC, it ranges from 0.2×10^{-13} to 4.1×10^{-13} m^2/s, based on the W/B, curing regime, medium solution concentration, steel fibre volume and testing age [150]. It is noteworthy that the chloride ion diffusion coefficient of UHPC is one point of magnitude lower than that of conventional concrete (CC) [171,172]. The chloride ion diffusion coefficients of C30, C80 and UHPC were also mentioned by [173], which are 1.1×10^{-13}, 6.0×10^{-13} and 0.2×10^{-13} m^2/s, respectively.

6.3. Corrosion of Steel Reinforcement

It is obvious that UHPC has a very low chloride ion permeability and therefore a high corrosion resistance [150]. An accelerated corrosion test was conducted to assess the corrosion rate of steel bars in high-performance concrete (HPC) and UHPC. The results indicated that the time to crack formation in UHPC was more than half the time observed in HPC [174]. Also, the rate of corrosion for steel bars in UHPC was described as 0.01 lm/year, which is quite lower than the permissible value of 1 lm/year [173]. In 2022, Kravanja et al. [160] presented the concept of a green superhydrophobic hybridization concrete that has anticorrosive properties.

6.4. Freeze–Thaw Resistance

Typically, freeze–thaw action in concrete leads to random cracking, surface scaling and joint deterioration due to D-cracking [150,175,176], leaving the structure with very low mechanical properties and permeability resistance. HPC possesses excellent freeze–thaw resistance due to its highly impermeable matrix with reduced capillary porosity [150,177–179]. Many researchers have discovered that after 300 or 600 freeze–thaw cycles, UHPC exhibited no deterioration [93,150]. Kravanja et al. also revealed that by applying superhydrophobic concrete, freeze–thaw damages may be reasonably decreased, and concrete shows high resistance against the freeze–thaw action [160].

6.5. Fire Resistance

Due to its low thermal conductivity and high thermal capacity, high fire resistance is one of the most important properties of concrete as a building material. If the free moisture content in the concrete is below 3–4%, explosive spalling in CC is unlikely to occur [150].

It is reported that UHPC samples exhibit a lower temperature difference between inner and outer layers than CC and HPC samples. However, spalling and loss of lower mass occur when the temperature reaches 800–900 °C [180,181].

Recently, one study revealed that UHPC with Macro Basalt Fibre (MBF) exhibited enhanced spalling resistance and higher mechanical properties at 400 °C and 500 °C compared to UHPC with steel fibres [122].

6.6. Nanotechnology

The significant progress in nanotechnology has opened up avenues for the effective use of various nanoscale materials, each endowed with distinctive characteristics. The substantial advancements in nanotechnology and nanomaterials have led to the integration of new properties directly into the fundamental structure of materials, thereby resulting in further enhancements [14].

The performance of modified concrete composites is influenced by the integration of nanomaterials. Strength and durability can be improved using nanomaterials in conjunction

with modified cement binders [182]. Therefore, a significant reduction in service and maintenance costs is expected [183].

Generally, nanoparticles are classified into two categories; Figure 7 depicts nanoparticles classifications.
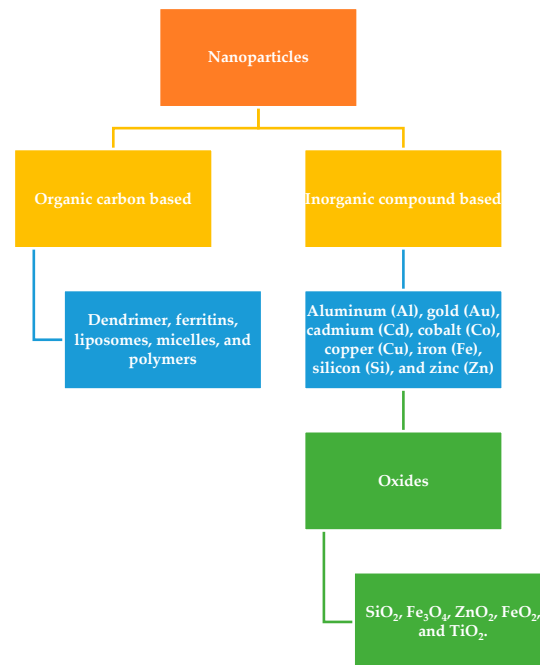
Figure 7. Nanoparticles classifications.

Several studies have been conducted to investigate the impact of different nanoparticles on modified cement materials. In a recent study, nano-silica (NS) and C-S-H seeds were incorporated into the UHPC mix. The results indicated a substantial increase in compressive strength, with a 457% improvement when 0.3% of NS was used and a 25% enhancement when C-S-H seeds were employed, compared to the reference sample [184].

Different nanoparticles affect the mixture in different ways; some nanomaterials enhance the mechanical properties of the UHPC mix, while at the same time affecting the freshness properties. For example, nano-silica is a widely used nanomaterial in modified-cement mixtures, typically ranging from 1% to 6%. Nano-silica can also reduce the flowability and setting time of the mixture, with maximum a reduction observed at 58% and 60%, respectively [14,185–201].

Various studies have revealed more or less similar characteristics of other nanoparticles, such as nano-titanium, nano-zinc, nano-clay, nano-aluminium, nano-iron, nano-glass, nano-zirconium, nano-copper and carbon nanotubes [14,192,202–214].

Nanoparticles not only enhance the mechanical and fresh properties of concrete but also contribute to making UHPC a multifunctional material. Silicon dioxide, for example, has the property of preventing the carbonization of concrete. In addition, the addition of titanium or titanium dioxide (TiO_2) to the mixture imparts self-cleaning properties to the concrete and enables it to absorb pollution. Silica and SF help to transform concrete into a self-compacting and rapidly hardening material. Carbon nanotubes play a role in minimizing the shrinkage of concrete [215].

7. Environmental Impact of UHPC: Life-Cycle Assessment and Sustainable Practices

Concrete, as a widely used construction material, has a substantial global environmental impact. Cement production, a key component of concrete, is responsible for approximately 7% of the total CO_2 emissions worldwide [216].

The fabrication of UHPC is also coupled with increased CO_2 emissions, which therefore have a negative impact on the environment. For this reason, the assessment procedure should integrate life-cycle assessment (LCA), a vast and standard method for evaluating the environmental impacts of assets and life-cycle cost, etc. [217].

LCA is a methodology that calculates the environmental impact of any building/structure throughout its entire life cycle (from its creation to its end of its life) [216,218]. In general, operation and maintenance (O & M) costs of a building are directly related to the initial costs invested. Lower initial costs usually lead to higher O & M costs and higher initial costs can lead to lower O & M costs. Figure 8 explains the structure of LCA. Typically, we can divide the entire procedure into two parts as shown in Figure 9 below.
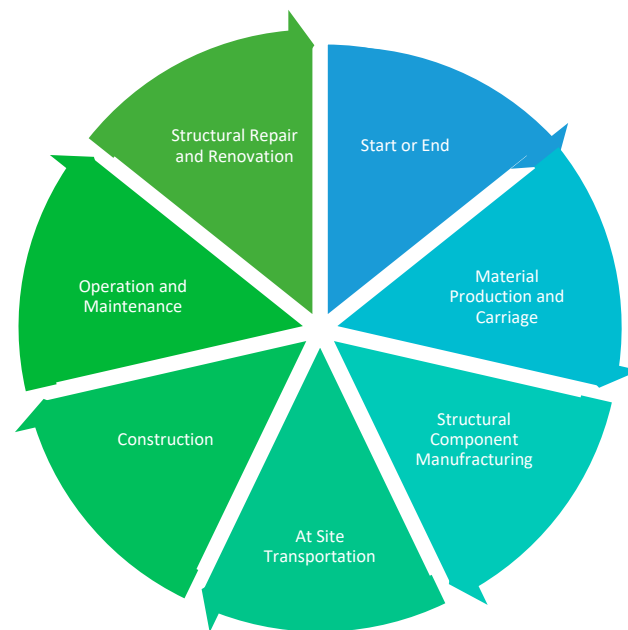
Figure 8. Typical life-cycle assessment framework.
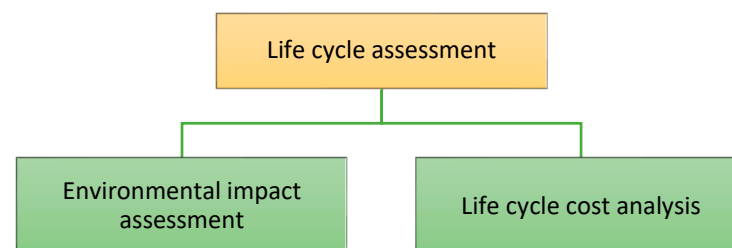
Figure 9. The environmental assessment and life-cycle analysis divisions.

7.1. Environmental Impact Assessment (EIA)

The environmental impact assessment procedure is based on various indicators, which are shown in Figure 10.

The accumulative environmental impact, measured in terms of CO_2 emissions, represents the global warming potential of the infrastructure throughout its service life. The initial phase involves the material formulation process, starting from raw material mining, transportation, etc. CO_2 emissions may be computed by multiplying the impact coupled with every raw material, which keeping in view the quantity of each [219].
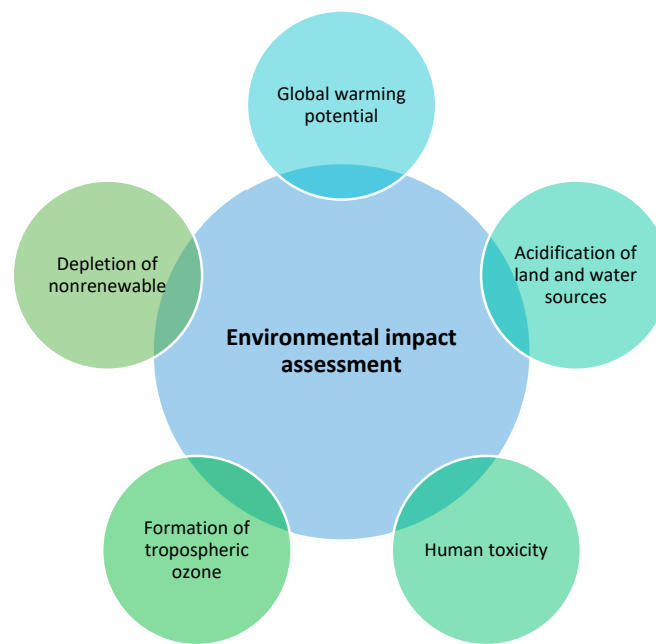
Figure 10. Environmental impact assessment indicators.

In this way, CO_2 emissions for any building/structure can be calculated by summing the unit CO_2 emissions weighted by the volume of all the materials involved in the structure. Therefore, the CO_2 emissions of all the materials at the manufacturing level can be calculated by Equation (5) [220].

$$EN_{manu} = \sum_{i=1}^{n_m} en_i \cdot V_i \tag{5}$$

In the above equation, n_m represents the number of different materials used within the under-consideration structure, en_i stands for the CO_2 emissions of a unit of the *i*-th material (kg-CO_2/m^3) in the manufacturing phase and V_i is the volume of each material, e.g., concrete, reinforcing steel, timber, etc.

The unit CO_2 emissions for different materials are influenced by several factors. Several industrial variables can influence the value of CO_2 emissions in the manufacturing phase [216]. The unit carbon CO_2 emission of a unit of concrete (kg-CO_2/m^3) in the production phase, $en_{c,manu}$, can be calculated using Equation (6).

$$en_{c,manu} = \sum_{i=1}^{n_{cm}} ma_i \cdot cefm_i \tag{6}$$

where ma_i is the quantity of the basic materials utilised in the production of one cubic meter of concrete (kg/m^3), n_{cm} is the number of batches for one cubic meter of concrete and $cefm_i$ is the CO_2 emission factor for the production of the *i*-th basic material (kg-CO_2/kg). In this context, the basic ingredients of UHPC are cement, silica fume, fibres, water and HRWR [216].

The environmental impact assessment of the transportation phase includes the CO_2 emissions released during the transportation of materials or other things from the plant/unit/factory to the site, depending on the distance and type of transportation. It can be calculated as follows.

$$EN_{trans} = \sum_{i=1}^{n_m} bma_i \cdot V_i \cdot \frac{d_i}{f_e} \cdot ceft \tag{7}$$

In Equation (7), bma_i represents the unit weight of the *i*-th material (kg/m^3) used in a structure, V_i is the volume of each *i*-th material (m^3), d_i is the transportation distance of the *i*-th material (km), f_e refers to the fuel efficiency (km/L) and $ceft$ is the CO_2 emission factor associated with the transportation of fuel consumption (CO_2 kg/L-kg).

The construction phase, which is included in the environmental impact assessment, is generally related to the construction techniques. For example, different types of equipment are used in different construction techniques, resulting in different energy efficiency and environmental impacts. In general, electricity consumption is considered as an environmental impact in this phase [219].

The next phase of the environmental impact assessment is the maintenance, repair and rehabilitation (MR&R) phase. This phase is basically divided into two main categories: preventive maintenance and essential maintenance. Preventive maintenance actions can be carried out either at regular or irregular intervals to prevent the structure from damage or deterioration, while essential maintenance measures are carried out when the performance indicator of the structure reaches the specified target value. The CO_2 emissions at this stage for the environmental impact assessment are directly related to the process or technique used for the rehabilitation of the structure and can be calculated using the following formula [216].

$$E_{main} = \sum_{i=1}^{n} E_{env,ini} \cdot r_{mi} \tag{8}$$

In Equation (8), n refers to the number of maintenance actions within the life-cycle, $E_{env,ini}$ represents the initial CO_2 emissions associated with manufacturing and transportation, and r_{mi} is the ratio of the CO_2 emissions of the i-th maintenance action to the CO_2 emissions of $E_{env,ini}$.

The final phase is the "end of life phase", which leads either to demolition of the building/structure or to material treatment or recycling of the material process and coupled transportation. The advantage for the environment is always hidden in recycling or material recovery [219].

7.2. Life-Cycle Cost Analysis and Equivalent Annual Cost (LCCA)

Similar to the EIA mentioned above, the LCCA also considers the entire life cycle of the building/structure from planning to demolition in relation to the invested costs. Therefore, LCCA is a decision support method that allows a comparative study of the life-cycle costs of alternatives that fulfil a similar function but differ significantly in a life-cycle terms [221]. The total cost during the lifetime of a building/structure can be calculated using Equation (9) [220].

$$LCC_{NPV} = C_{cons} + \sum_{j=1}^{n_{ins}} \frac{C_{ins,j}(t_j)}{(1+r)^{t_j}} + \sum_{k=1}^{n_{mt}} \frac{C_{mt,k}(t_k)}{(1+r)^{t_k}} + \sum_{i=1}^{n_{fe}} \frac{C_{fc,i}(t_i)}{(1+r)^{t_i}} + \frac{C_{dm}}{(1+r)^T} - \frac{R_v}{(1+r)^T} \tag{9}$$

In Equation (9), r is the monetary discount rate used to discount future cash flows to their present value; C_{cons} are the initial construction costs, including material and labour costs; C_{ins} are the inspection costs; C_{mt} are the maintenance costs, which include both direct and indirect costs for maintenance activities; C_{fc} are the failure costs, which include both direct and indirect costs due to structural failure; C_{dm} are the demolition costs, including the costs of destruction, reclaim and recycling; R_v is the residual monetary value of the structure at the end of its design service life, assuming it does not collapse; T is the investigated life cycle, such as the designed service life, n_{ins}, n_{mt} and n_{fe} represent the times of inspection, maintenance, and failure events, respectively, during the investigated life cycle.

In order to calculate the life-cycle costs, we must first determine the "initial construction costs", which can be calculated using Equation (10).

$$C_{cons} = \sum_{i}^{n_m} C_{m,i} \cdot V_i \cdot \rho_i \tag{10}$$

In the above equation, n_m is the number of different materials used in a building/structure, c_{mi} is the unit price per ton of the i-th material, V_i is the total volume of the i-th material and ρ_i is the density of the i-th material.

To address this issue, the method of equivalent annual cost should be employed as an additional performance indicator for comparing assets with different service lives [222,223]. The equivalent uniform annual costs LCC_{EUAC} can be calculated using Equation (11) [216].

$$LCC_{EUAC} = \begin{cases} LCC_{NPV} \cdot r \cdot \frac{(1+r)^T}{(1+r)^T - 1}, & r > 0 \\ \frac{LCC_{NPV}}{T}, & r = 0 \end{cases} \tag{11}$$

where LCC_{NPV} is the net present value for life-cycle and cost analysis, r is the monetary discount rate and T is the investigated life cycle.

7.3. Numerical Examples for the Determination of CO_2 Emissions

Three numerical examples of three different mixtures for calculating CO_2 emissions in the production of one cubic meter of UHPC are shown in Table 5. Using Equation (6), the first UHPC mixture mixed for a bridge in China [216] has 877 kg emissions of CO_2/m^3; the second mixture, U0.20F2.5, mixed with fly ash and aeolian sand [224], exhibits 852 kg emissions of CO_2/m^3; and the third mixture with fly ash, and silica powder and sand, used for a bridge in Vietnam [225], shows 1146 kg-CO_2/m^3. In Table 5, each mixture is presented in two separate columns with the weights of the materials used and their unit CO_2 emissions. In terms of CO_2 emissions, cement is the most polluting material. If only the contribution of cement is calculated, it amounts to 692 kg-CO_2/m^3 (79%) of the total CO_2 emissions for the first mixture, 538 kg-CO_2/m^3 (63%) for the second mixture and 887 kg-CO_2/m^3 (77%) for the third mixture. Note that the second mixture exhibits a lower percentage of CO_2 emissions from cement compared to the first and third mixtures, as a lower content of cement is mixed, and a higher unit CO_2 emission of steel fibre is used.

Table 5. CO_2 emission in production 1 m^3 of UHPC.

| Material	Reference [216]		Reference [224]		Reference [225]	
	Weight (kg)	Unit CO$_2$ Emission (kg-CO$_2$/kg)	Weight (kg)	Unit CO$_2$ Emission (kg-CO$_2$/kg)	Weight (kg)	Unit CO$_2$ Emission (kg-CO$_2$/kg)
Cement	800	0.865	646	0.8324	1025	0.8650
Fly ash	-	-	323	0.0090	175	0.1965
Silica fume	250	0	108	0	330	0.0070
Silica powder	-	-	-	-	300	0.0018
Silica sand	-	-	-	-	650	0.0009
Aeolian sand	-	-	862	0.0010	-	-
Aggregate	750	0.0013	-	-	-	-
Steel fibre	195	0.94	195	1.4965	235	0.9299
Water	200	-	215	0.0003	246	-
Superplasticizer	40	0.0184	22	0.7200	31	0.092
Expensive agent	-	-	32	0.0810	-	-
CO$_2$ emissions/m^3	877 kg-CO$_2$/m^3		852 kg-CO$_2$/m^3		1146 kg-CO$_2$/m^3	

8. Applications of UHPC

The properties of UHPC such as strength, ductility, durability and aesthetic design flexibility, make it a smart material. Thanks to these unique properties of UHPC, various tasks can be achieved, such as load-bearing elements with thinner cross-sections (comparable to steel profiles), curved and more complex and sophisticated shapes [167]. According to Grand View Research (GVR), the global market for UHPC was estimated at USD 892 million in 2016 and is expected to grow by 8.6% to USD 1867.3 million by 2025 [11]. The following subsections present some very well-known structural applications of UHPC.

8.1. Buildings

In 2013, the building of the "Museum of European and Mediterranean Civilizations" was constructed in Marseille, France, with extensive use of UHPC [226]. In 2014, the "foundation Louis Vuitton pour la Creation" was built in Paris, France, with complex geometric features. The roof of the "Jean Bouin Stadium" in Paris was also built with UHPC [226,227]. In Switzerland, UHPC was used for the roof of the Olympic Museum

in Lausanne [228]. The façade of the National Museum of Qatar was built with UHPC and opened to the public in 2019 [226]. In addition, some UHPC buildings are shown in Figure 11.
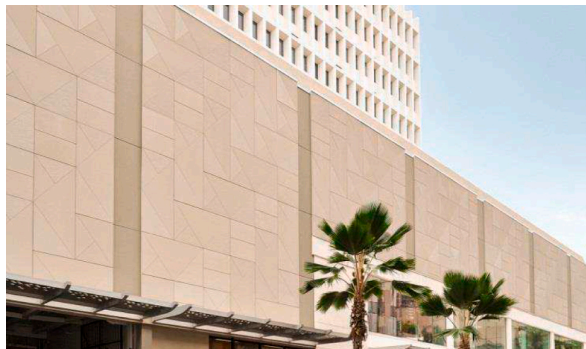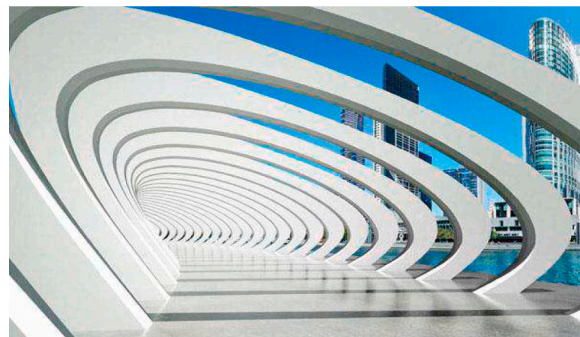

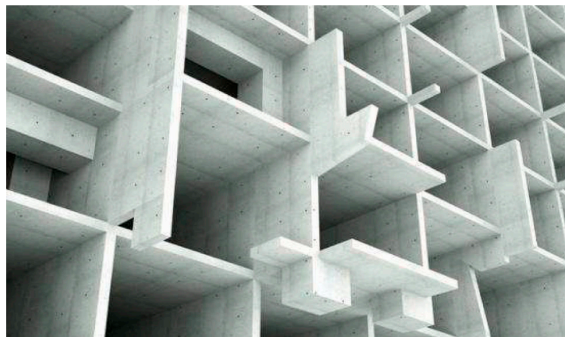(**a**) Waikiki Business Plaza, Honolulu, USA.

(**b**) Rabat-Sale Airport, Morocco.

(**c**) Woodsy Park Pavilion, Toronto, Canada.

(**d**) Sitrad Elite Benton Ltd., Casablanca, Morocco.

(**e**) BDAS's building solution, Bangladesh.

(**f**) The world's first UHPC pedestrian cable-stayed bridge.

Figure 11. Typical UHPC building structures [19].

8.2. Bridges

In 1997, UHPC was used for the first time in the construction of a pedestrian bridge in Quebec, Canada. In 2000, UHPC became commercially available in the United States and the first UHPC girder bridge, known as the "Mars Hill Bridge", was built in Wapello County, Iowa [226].

In Malaysia, almost 113 UHPC bridges have been completed or are still under construction since 2010. One of the completed bridges in Malaysia, located in Perak, is shown in Figure 12. After the successful completion of these pedestrian bridges, UHPC pedestrian bridges were also built in Europe, North America, Asia and Australia [19].

In 2005, the first four road bridges were built with UHPC: the "Shepherd's Gully Bridge" in Australia, the "Bourd-les-Valence Bridge" in France, the "Horikoshi C-ramp Bridge" in Japan, and the mentioned "Mars Hill Bridge" in Wapello Country Iowa USA [11].
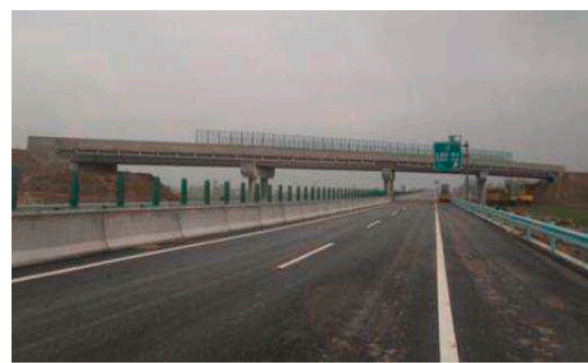
(**a**) Mars Hill Bridge, Wapelo, USA.
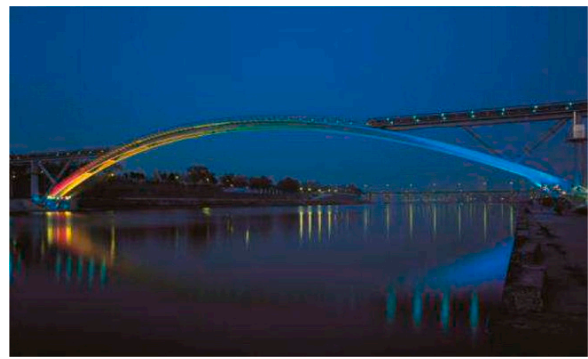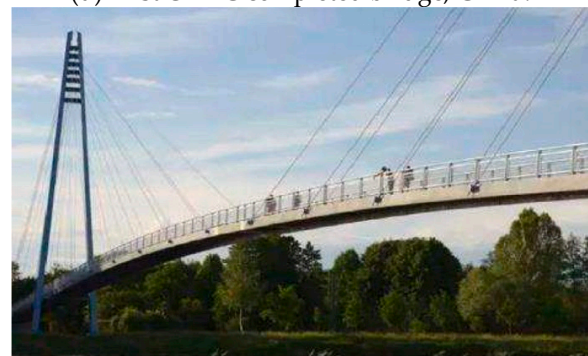

(**b**) Foot Bridge of Peace in Seoul, Korea.

(**c**) Sakata-Mirai Bridge, Sakata, Japan.

(**d**) First UHPC completed bridge, China.

(**e**) Kampung Linsum Bridge, N. Sembilan, Malaysia.

(**f**) Celakovice pedestrian bridge, Czech Republic.

Figure 12. UHPC bridges [19].

In 2013, the United States Federal Highway Administration (FHWA) published a report stating that 55 bridges were built with UHPC in the USA and Canada, 22 in Europe, and 27 in Asia and Australia [229]. It is also reported that UHPC is actively used in the repair of bridge beams, bridge decks, bridge piles and wind turbine towers [230].

In addition to the successful applications of UHPC in buildings, bridges, and wind turbine towers, an experimental study investigated the durability of UHPC in a harsh marine environment over 21 years. The results showed that the durability of UHPC in harsh marine environments is significantly higher than that of conventional high-performance concrete (HPC) and normal concrete, regardless of the curing process. Chloride penetration was found to occur to a depth of about 10 mm regardless of the exposure time [230]. Only recently, a successful experiment was conducted in India to produce a green approach for railroad sleepers made of ternary, blended prestressed cement concrete railway sleepers [231].

9. Conclusions and Future Perspectives

The review article reports on the progress and applications of ultra-high-performance concrete (UHPC). The article comprehensively addresses the historical development of UHPC, its production and the design aspects encompassing composition and methodology. It delves into the mechanical properties of UHPC, recent innovations and ongoing research. Topics such as multifunctionality, nanotechnology, durability assessment, environmental impact, life-cycle cost analysis, a numerical example for determining CO_2 emissions and diverse applications in buildings and bridges are thoroughly discussed.

Research and innovation in the field of ultra-high-performance concrete (UHPC) have made it an innovative material with exceptional mechanical strength, durability and multifunctionality. Remarkable properties such as low porosity, high packing density and minimal permeability make UHPC stand out in comparison to conventional concrete. The incorporation of steel fibres enhances tensile and flexural strengths, shifting the failure patterns from brittle to ductile. However, challenges, including production costs and mixer failures in large-scale operations, remain. The use of supplementary cementitious materials such as fly ash, rice husk ash and metakaolin contributes to sustainability but faces challenges related to the different chemical compositions. Basalt fibres, thermally treated sugar cane bagasse ash, and rice husk ash emerge as promising alternatives with better mechanical properties. The integration of nanotechnology, such as nano-silica and other nanoparticles, has a significant impact on the properties of UHPC. While these nanoparticles improve the mechanical strength, they also affect the freshness properties, which requires careful consideration when developing the mix. In addition, UHPC shows promising progress as a smart and multifunctional material, offering capabilities such as superhydrophobicity, self-sensing, self-heating and self-luminescence.

The focus of further research and activities in UHPC should be on improving environmental impact and sustainability, implementing real cost reduction strategies, fostering innovations and exploring opportunities for global market expansion. To summarize:

- It is imperative to minimize the environmental footprint of UHPC production. Exploring sustainable alternatives, recycling methods and environmentally friendly components will improve the overall environmental profile.
- Overcoming the challenges of large-scale production is crucial for the wide acceptance of UHPC. Solving problems related to mixer failures and optimizing production processes can pave the way for wider application in construction projects.
- Developing cost-effective formulations without compromising performance is essential. Exploring alternative materials and production techniques may contribute to reducing the overall cost of UHPC, making it more accessible for various construction projects.
- Further research into the effects of different nanoparticles on the properties of UHPC is warranted. Understanding the interaction mechanisms and optimizing the nanomaterial content can lead to improved mechanical and fresh properties.
- Investigating the use of waste materials from different industries, such as the perfume or geranium industry, can contribute to sustainable and environmentally conscious UHPC practices. This can provide valuable insights into novel waste materials that can improve the performance of UHPC.
- Extending life-cycle assessments (LCAs) to comprehensively evaluate the environmental impact of UHPC throughout its entire life cycle is crucial. Incorporating LCA considerations into material selection and production processes can lead to sustainable practices.
- With a high projected growth rate, the UHPC market is expected to expand globally. Ongoing research, coupled with successful applications in real-world projects, is likely to increase adoption and have a greater impact on the construction industry.

Addressing challenges and exploring innovative solutions will contribute to the continued growth and sustainable integration of UHPC in various construction applications, including bridges, buildings, marine structures, military applications, wind turbine tow-

ers, railroad components, water and wastewater infrastructure, tunnels, smart concrete applications, noise barriers and custom architectural elements.

References

1. *C1856/C1856M-17*; Standard Practice for Fabricating and Testing Specimens of Ultra-High Performance Concrete. ASTM: West Conshohocken, PA, USA, 2017.
2. FHWA. *Properties and Behavior of UHPC-Class Materials*; FHWA: Georgetown Pike, VA, USA, 2018; pp. 1–153.
3. El-Tawil, S.; Tai, Y.-S.; Belcher, J.A., II; Rogers, D. Open-Recipe Ultra-High-Performance Concrete. *CI Concr. Int.* **2020**, *42*, 53–57.
4. Wu, Z.; Shi, C.; He, W.; Wu, L. Effects of steel fiber content and shape on mechanical properties of ultra high performance concrete. *Constr. Build. Mater.* **2016**, *103*, 8–14. [CrossRef]
5. Su, Y.; Li, J.; Wu, C.; Wu, P.; Li, Z.X. Effects of steel fibres on dynamic strength of UHPC. *Constr. Build. Mater.* **2016**, *114*, 708–718. [CrossRef]
6. Linmei, W.U. Study on dimensional stability of ultra high performance. Ph.D. Thesis, University of Southern Queensland, Darling Heights, QLD, Australia, 2020.
7. Zhou, M.; Wu, Z.; Ouyang, X.; Hu, X.; Shi, C. Mixture design methods for ultra-high-performance concrete—A review. *Cem. Concr. Compos.* **2021**, *124*, 104242. [CrossRef]
8. Park, S.; Lee, N.; An, G.-H.; Koh, K.-T.; Ryu, G.-S. Modeling the Effect of Alternative Cementitious Binders in Ultra-High-Performance Concrete. *Materials* **2021**, *14*, 7333. [CrossRef] [PubMed]
9. Schmidt, M.; Fehling, E. Ultra High Performance Concrete: Research, Development and Application in Europe. *Am. Concr. Inst. ACI Spec.* **2005**, *228*, 51–77.
10. Shi, C.; Wu, Z.; Xiao, J.; Wang, D.; Huang, Z.; Fang, Z. A review on ultra high performance concrete: Part I. Raw materials and mixture design. *Constr. Build. Mater.* **2015**, *101*, 741–751. [CrossRef]
11. Azmee, N.M.; Shafiq, N. Ultra-high performance concrete: From fundamental to applications. *Case Stud. Constr. Mater.* **2018**, *9*, e00197. [CrossRef]
12. Song, F.; Li, Q.; Xu, S. A review of self-sensing ultra-high performance concrete: Towards next-generation smart structural materials. *Cem. Concr. Compos.* **2023**, *145*, 105350. [CrossRef]
13. El-Abbasy, A.A. Tensile, flexural, impact strength, and fracture properties of ultra-high-performance fiber-reinforced concrete—A comprehensive review. *Constr. Build. Mater.* **2023**, *408*, 133621. [CrossRef]
14. Huseien, G. A Review on Concrete Composites Modified with Nanoparticles. *J. Compos. Sci.* **2023**, *7*, 67. [CrossRef]
15. Fan, D.; Zhu, J.; Fan, M.; Lu, J.X.; Chu, S.H.; Dong, E.; Yu, R. Intelligent design and manufacturing of ultra-high performance concrete (UHPC)—A review. *Constr. Build. Mater.* **2023**, *385*, 131495. [CrossRef]
16. Ullah, R.; Qiang, Y.; Ahmad, J.; Vatin, N.I.; El-Shorbagy, M.A. Ultra-High-Performance Concrete (UHPC): A State-of-the-Art Review. *Materials* **2022**, *15*, 4131. [CrossRef] [PubMed]
17. Yang, J.; Chen, B.; Su, J.; Xu, G.; Zhang, D.; Zhou, J. Effects of Fibers on the Mechanical Properties of UHPC: A Review. *J. Traffic Transp. Eng. (Engl. Ed.)* **2022**, *9*, 363–387. [CrossRef]
18. Akeed, M.H.; Qaidi, S.; Ahmed, H.U.; Faraj, R.H.; Majeed, S.S.; Mohammed, A.S.; Emad, W.; Tayeh, B.A.; Azevedo, A.R.G. Ultra-high-performance fiber-reinforced concrete. Part V: Mixture design, preparation, mixing, casting, and curing. *Case Stud. Constr. Mater.* **2022**, *17*, e01265. [CrossRef]
19. Amran, M.; Huang, S.S.; Onaizi, A.M.; Makul, N.; Abdelgader, H.S.; Ozbakkaloglu, T. Recent trends in ultra-high performance concrete (UHPC): Current status, challenges, and future prospects. *Constr. Build. Mater.* **2022**, *352*, 129029. [CrossRef]
20. Shah, H.A.; Yuan, Q.; Photwichai, N. Use of materials to lower the cost of ultra-high-performance concrete—A review. *Constr. Build. Mater.* **2022**, *327*, 127045. [CrossRef]
21. Yoo, D.Y.; Oh, T.; Banthia, N. Nanomaterials in ultra-high-performance concrete (UHPC)—A review. *Cem. Concr. Compos.* **2022**, *134*, 104730. [CrossRef]

22. Wu, Y.; Dong, L.; Shu, X.; Yang, Y.; She, W.; Ran, Q. A review on recent advances in the fabrication and evaluation of superhydrophobic concrete. *Compos. B Eng.* **2022**, *237*, 109867. [CrossRef]

23. Wang, X.; Wu, D.; Zhang, J.; Yu, R.; Hou, D.; Shui, Z. Design of sustainable ultra-high performance concrete: A review. *Constr. Build. Mater.* **2021**, *307*, 124643. [CrossRef]

24. Park, S.; Wu, S.; Liu, Z.; Pyo, S. The role of supplementary cementitious materials (SCMs) in ultra high performance concrete (uhpc): A review. *Materials* **2021**, *14*, 1472. [CrossRef]

25. Du, J.; Meng, W.; Khayat, K.H.; Bao, Y.; Guo, P.; Lyu, Z.; Abu-obeidah, A.; Nassif, H.; Wang, H. New development of ultra-high-performance concrete (UHPC). *Compos. B Eng.* **2021**, *224*, 109220. [CrossRef]

26. Larsen, I.L.; Thorstensen, R.T. The influence of steel fibres on compressive and tensile strength of ultra high performance concrete: A review. *Constr. Build. Mater.* **2020**, *256*, 119459. [CrossRef]

27. Spasojević, A. Structural Implication of Ultra-High-Performance Fiber Reinforced Concrete in Bridges. Ph.D. Thesis, Swiss Federal Institute of Technology Lausanne, Lausanne, Switzerland, 2008.

28. Lei, L.; Hirata, T.; Plank, J. 40 years of PCE superplasticizers—History, current state-of-the-art and an outlook. *Cem. Concr. Res.* **2022**, *157*, 106826. [CrossRef]

29. Bache, H.H. Densified cement ultra-fine particle-based materials. In Proceedings of the International Conference on Superplasticizers in Concrete, Ottawa, ON, Canada, 10–12 June 1981.

30. Richard, P.; Cheyrezy, M. Composition of Reactive Powder Concretes. *Cem. Concr. Res.* **1995**, *25*, 1501–1511. [CrossRef]

31. Rossi, P.; Arca, A.; Parant, E.; Fakhri, P. Bending and compressive behaviours of a new cement composite. *Cem. Concr. Res.* **2005**, *35*, 27–33. [CrossRef]

32. Soliman, N.A. Development of UHPC Using Waste Glass Materials–Towards Innovative Eco-Friendly Concrete. Ph.D. Thesis, University Sherbrooke, Sherbrooke, QC, Canada, 2016.

33. Fehling, E.; Schmidt, M.; Walraven, J.; Leutbecher, T.; Froehlich, S. *Ultra-High Performance Concrete UHPC: Fundamentals, Design, Examples*, 1st ed.; Wilhelm Ernst & Sohn Verlag fur Architektur und Technische Wissenschaften: Berlin, Germany, 2014.

34. Blais, P.Y.; Couture, M. Precast, Prestressed Pedestrian Bridge World's First Reactive Powder Concrete Structure. *PCI J.* **1999**, *44*, 60–71. [CrossRef]

35. Zdeb, T. Ultra-high performance concrete-properties and technology. *Bull. Pol. Acad. Sci. Tech. Sci.* **2013**, *61*, 183–193. [CrossRef]

36. Abbas, S.; Soliman, A.M.; Nehdi, M.L. Exploring mechanical and durability properties of ultra-high performance concrete incorporating various steel fiber lengths and dosages. *Constr. Build. Mater.* **2015**, *75*, 429–441. [CrossRef]

37. Kang, S.H.; Jeong, Y.; Tan, K.H.; Moon, J. High-volume use of limestone in ultra-high performance fiber-reinforced concrete for reducing cement content and autogenous shrinkage. *Constr. Build. Mater.* **2019**, *213*, 292–305. [CrossRef]

38. Huang, H.; Gao, X.; Wang, H.; Ye, H. Influence of rice husk ash on strength and permeability of ultra-high performance concrete. *Constr. Build. Mater.* **2017**, *149*, 621–628. [CrossRef]

39. Meng, W.; Valipour, M.; Khayat, K.H. Optimization and performance of cost-effective ultra-high performance concrete. *Mater. Struct./Mater. Constr.* **2017**, *50*, 1–16. [CrossRef]

40. Zhang, H.; Ji, T.; He, B.; He, L. Performance of ultra-high performance concrete (UHPC) with cement partially replaced by ground granite powder (GGP) under different curing conditions. *Constr. Build. Mater.* **2019**, *213*, 469–482. [CrossRef]

41. Zhang, H.; Ji, T.; Zeng, X.; Yang, Z.; Lin, X.; Liang, Y. Mechanical behavior of ultra-high performance concrete (UHPC) using recycled fine aggregate cured under different conditions and the mechanism based on integrated microstructural parameters. *Constr. Build. Mater.* **2018**, *192*, 489–507. [CrossRef]

42. Korpa, A.; Kowald, T.; Trettin, R. Phase development in normal and ultra high performance cementitious systems by quantitative X-ray analysis and thermoanalytical methods. *Cem. Concr. Res.* **2009**, *39*, 69–76. [CrossRef]

43. Wang, C.; Yang, C.; Liu, F.; Wan, C.; Pu, X. Preparation of Ultra-High Performance Concrete with common technology and materials. *Cem. Concr. Compos.* **2012**, *34*, 538–544. [CrossRef]

44. Ding, M.; Yu, R.; Feng, Y.; Wang, S.; Zhou, F.; Shui, Z.; Gao, X.; He, Y.; Chen, L. Possibility and advantages of producing an ultra-high performance concrete (UHPC) with ultra-low cement content. *Constr. Build. Mater.* **2021**, *273*, 122023. [CrossRef]

45. Fládr, J.; Bílý, P.; Trtík, T. Analysis of the influence of supplementary cementitious materials used in UHPC on modulus of elasticity. *IOP Conf. Ser. Mater. Sci. Eng.* **2019**, *522*, 012010. [CrossRef]

46. Mo, Z.; Gao, X.; Su, A. Mechanical performances and microstructures of metakaolin contained UHPC matrix under steam curing conditions. *Constr. Build. Mater.* **2021**, *268*, 121112. [CrossRef]

47. Gu, C.; Sun, W.; Guo, L.; Wang, Q. Effect of curing conditions on the durability of ultra-high performance concrete under flexural load. *J. Wuhan Univ. Technol. Mater. Sci. Ed.* **2016**, *31*, 278–285. [CrossRef]

48. Wu, Z.; Shi, C.; He, W. Comparative study on flexural properties of ultra-high performance concrete with supplementary cementitious materials under different curing regimes. *Constr. Build. Mater.* **2017**, *136*, 307–313. [CrossRef]

49. Yazici, H.; Yiğiter, H.; Karabulut, A.Ş.; Baradan, B. Utilization of fly ash and ground granulated blast furnace slag as an alternative silica source in reactive powder concrete. *Fuel* **2008**, *87*, 2401–2407. [CrossRef]

50. Siddique, R.; Klaus, J. Influence of metakaolin on the properties of mortar and concrete: A review. *Appl. Clay Sci.* **2009**, *43*, 392–400. [CrossRef]

51. Peng, Y.; Hu, S.; Ding, Q. Preparation of reactive powder concrete using fly ash and steel slag powder. *J. Wuhan Univ. Technol. Mater. Sci. Ed.* **2010**, *25*, 349–354. [CrossRef]

52. Van Tuan, N.; Ye, G.; Van Breugel, K.; Copuroglu, O. Hydration and microstructure of ultra high performance concrete incorporating rice husk ash. *Cem. Concr. Res.* **2011**, *41*, 1104–1111. [CrossRef]

53. Van, V.; Ludwig, H. Proportioning optimization of UHPC containing rice husk ash and ground granulated blast-furnace slag. In Proceedings of the 3rd International Symposium on UHPC and Nanotechnology for High Performance Construction Materials, Kassel, Germany, 7–9 March 2012.

54. *ASTM C618-99*; Standard Specification for Coal Fly Ash and Raw or Calcined Natural Pozzolan for Use as a Mineral Admixture in Concrete. ASTM: West Conshohocken, PA, USA, 2021.

55. Yazici, H.; Yardimci, M.Y.; Yiğiter, H.; Aydin, S.; Türkel, S. Mechanical properties of reactive powder concrete containing high volumes of ground granulated blast furnace slag. *Cem. Concr. Compos.* **2010**, *32*, 639–648. [CrossRef]

56. Soliman, N.A.; Tagnit-Hamou, A. Partial substitution of silica fume with fine glass powder in UHPC: Filling the micro gap. *Constr. Build. Mater.* **2017**, *139*, 374–384. [CrossRef]

57. Taha, B.; Nounu, G. Utilizing Waste Recycled Glass as Sand/Cement Replacement in Concrete. *J. Mater. Civ. Eng.* **2009**, *21*, 709–721. [CrossRef]

58. Tafraoui, A.; Escadeillas, G.; Lebaili, S.; Vidal, T. Metakaolin in the formulation of UHPC. *Constr. Build. Mater.* **2009**, *23*, 669–674. [CrossRef]

59. Bentz, D.P.; Ferraris, C.F.; Jones, S.Z.; Lootens, D.; Zunino, F. Limestone and silica powder replacements for cement: Early-age performance. *Cem. Concr. Compos.* **2017**, *78*, 43–56. [CrossRef]

60. Fanghui, H.; Qiang, W.; Mutian, L.; Yingjun, M. Early hydration properties of composite binder containing limestone powder with different finenesses. *J. Therm. Anal. Calorim.* **2016**, *123*, 1141–1151. [CrossRef]

61. Scrivener, K.; Martirena, F.; Bishnoi, S.; Maity, S. Calcined Clay Limestone Cements (LC^3). *Cem. Concr. Res.* **2018**, *114*, 49–56. [CrossRef]

62. Yang, R.; Yu, R.; Shui, Z.; Gao, X.; Xiao, X.; Fan, D.; Chen, Z.; Cai, J.; Li, X.; He, Y. Feasibility analysis of treating recycled rock dust as an environmentally friendly alternative material in Ultra-High Performance Concrete (UHPC). *J. Clean. Prod.* **2020**, *258*, 120673. [CrossRef]

63. Xue, G.; Yilmaz, E.; Song, W.; Cao, S. Mechanical, flexural and microstructural properties of cement-tailings matrix composites: Effects of fiber type and dosage. *Compos. B Eng.* **2019**, *172*, 131–142. [CrossRef]

64. Zhang, Y.; Zhu, Y.; Qu, S.; Kumar, A.; Shao, X. Improvement of flexural and tensile strength of layered-casting UHPC with aligned steel fibers. *Constr. Build. Mater.* **2020**, *251*, 118893. [CrossRef]

65. Hung, C.C.; Lee, H.S.; Chan, S.N. Tension-stiffening effect in steel-reinforced UHPC composites: Constitutive model and effects of steel fibers, loading patterns, and rebar sizes. *Compos. B Eng.* **2019**, *158*, 709–721. [CrossRef]

66. Wu, Z.; Shi, C.; He, W.; Wang, D. Static and dynamic compressive properties of ultra-high performance concrete (UHPC) with hybrid steel fiber reinforcements. *Cem. Concr. Compos.* **2017**, *79*, 148–157. [CrossRef]

67. Banthia, N.; Foy, C. Marine Curing of Steel Fiber Composites. *J. Mater. Civ. Eng.* **1989**, *1*, 86–96. [CrossRef]

68. Fan, L.; Meng, W.; Teng, L.; Khayat, K.H. Effect of steel fibers with galvanized coatings on corrosion of steel bars embedded in UHPC. *Compos. B Eng.* **2019**, *177*, 107445. [CrossRef]

69. Meng, W.; Khayat, K.H. Effect of Hybrid Fibers on Fresh Properties, Mechanical Properties, and Autogenous Shrinkage of Cost-Effective UHPC. *J. Mater. Civ. Eng.* **2018**, *30*, 04018030. [CrossRef]

70. Yu, R.; Spiesz, P.; Brouwers, H.J.H. Mix design and properties assessment of Ultra-High Performance Fibre Reinforced Concrete (UHPFRC). *Cem. Concr. Res.* **2014**, *56*, 29–39. [CrossRef]

71. Ilg, M.; Plank, J. Non-adsorbing small molecules as auxiliary dispersants for polycarboxylate superplasticizers. *Colloids Surf. A Physicochem. Eng. Asp.* **2020**, *587*, 124307. [CrossRef]

72. Stovall, T.; de Larrard, F.; Buil, M. Linear Packing Density Model of Grain Mixtures. *Powder Technol.* **1986**, *48*, 1–12. [CrossRef]

73. de Larrard, F.; Sedran, T. Optimization of Ultra-High-Performance Concrete by the Use of a Packing Model. *Cem. Concr. Res.* **1994**, *24*, 997–1009. [CrossRef]

74. de Larrard, F.; Sedran, T. Mixture-Proportioning of High-Performance Concrete. *Cem. Concr. Res.* **2002**, *32*, 1699–1704. [CrossRef]

75. Fennis, S.A.A.M.; Walraven, J.C.; den Uijl, J.A. Compaction-Interaction Packing Model: Regarding the Effect of Fillers in Concrete Mixture Design. *Mater. Struct.* **2013**, *46*, 463–478. [CrossRef]

76. Fuller, W.B.; Thompson, S.E. The Laws of Proportioning Concrete. *Trans. Am. Soc. Civ. Eng.* **1907**, *59*, 67–143. [CrossRef]

77. Brouwers, H.J.H.; Radix, H.J. Self-Compacting Concrete: Theoretical and Experimental Study. *Cem. Concr. Res.* **2005**, *35*, 2116–2136. [CrossRef]

78. Li, L.G.; Kwan, A.K.H. Packing Density of Concrete Mix under Dry and Wet Conditions. *Powder Technol.* **2014**, *253*, 514–521. [CrossRef]

79. Graybeal, B. *Ultra-High Performance Concrete (FHWA-HRT-11-038)*; Federal Highway Administration: Washington, DC, USA, 2011.

80. Teng, L.; Meng, W.; Khayat, K.H. Rheology control of ultra-high-performance concrete made with different fiber contents. *Cem. Concr. Res.* **2020**, *138*, 106222. [CrossRef]

81. Yu, R.; Spiesz, P.; Brouwers, H.J.H. Development of an eco-friendly Ultra-High Performance Concrete (UHPC) with efficient cement and mineral admixtures uses. *Cem. Concr. Compos.* **2015**, *55*, 383–394. [CrossRef]

82. He, J.; Chen, W.; Zhang, B.; Yu, J.; Liu, H. The Mechanical Properties and Damage Evolution of UHPC Reinforced with Glass Fibers and High-Performance Polypropylene Fibers. *Materials* **2021**, *14*, 2455. [CrossRef]

83. Chen, H.-J.; Yu, Y.-L.; Tang, C.-W. Mechanical Properties of Ultra-High Performance Concrete before and after Exposure to High Temperatures. *Materials* **2020**, *13*, 770. [CrossRef]

84. Khatib, J.M. Metakaolin Concrete at a Low Water to Binder Ratio. *Constr. Build. Mater.* **2008**, *22*, 1691–1700. [CrossRef]

85. Abdellatief, M.; AL-Tam, S.M.; Elemam, W.E.; Alanazi, H.; Elgendy, G.M.; Tahwia, A.M. Development of Ultra-High-Performance Concrete with Low Environmental Impact Integrated with Metakaolin and Industrial Wastes. *Case Stud. Constr. Mater.* **2023**, *18*, e01724. [CrossRef]

86. Tafraoui, A.; Escadeillas, G.; Vidal, T. Durability of the Ultra High Performances Concrete containing metakaolin. *Constr. Build. Mater.* **2016**, *112*, 980–987. [CrossRef]

87. Song, Q.; Yu, R.; Shui, Z.; Wang, Y.; Rao, S.; Wu, S.; He, Y. Physical and chemical coupling effect of metakaolin induced chloride trapping capacity variation for Ultra High Performance Fibre Reinforced Concrete (UHPFRC). *Constr. Build. Mater.* **2019**, *223*, 765–774. [CrossRef]

88. Xie, H.; Yang, L.; Li, J.; Chen, Z.; Zhang, F.; Liu, Y.; Sui, Z.; Zhang, Q. Research on Mode-I Fracture Characteristics of Basalt Fiber Reactive Powder Concrete. *J. Build. Eng.* **2023**, *80*, 108159. [CrossRef]

89. Kočí, V.; Vejmelková, E.; Koňáková, D.; Pommer, V.; Grzeszczyk, S.; Matuszek-Chmurowska, A.; Mordak, A.; Černý, R. Basic physical, mechanical, thermal and hygric properties of reactive powder concrete with basalt and polypropylene fibers after high-temperature exposure. *Constr. Build. Mater.* **2023**, *374*, 130922. [CrossRef]

90. AlAteah, A.H. Engineering Characteristics of Ultra-High Performance Basalt Fiber Concrete Incorporating Geranium Plant Waste. *Case Stud. Constr. Mater.* **2023**, *19*, e02618. [CrossRef]

91. Yang, L.; Shi, C.; Liu, J.; Wu, Z. Factors affecting the effectiveness of internal curing: A review. *Constr. Build. Mater.* **2021**, *267*, 121017. [CrossRef]

92. Li, W.; Huang, Z.; Hu, G.; Hui Duan, W.; Shah, S.P. Early-age shrinkage development of ultra-high-performance concrete under heat curing treatment. *Constr. Build. Mater.* **2017**, *131*, 767–774. [CrossRef]

93. Alkaysi, M.; El-Tawil, S.; Liu, Z.; Hansen, W. Effects of silica powder and cement type on durability of ultra high performance concrete (UHPC). *Cem. Concr. Compos.* **2016**, *66*, 47–56. [CrossRef]

94. Yunsheng, Z.; Wei, S.; Sifeng, L.; Chujie, J.; Jianzhong, L. Preparation of C200 green reactive powder concrete and its static-dynamic behaviors. *Cem. Concr. Compos.* **2008**, *30*, 831–838. [CrossRef]

95. Yang, S.L.; Millard, S.G.; Soutsos, M.N.; Barnett, S.J.; Le, T.T. Influence of aggregate and curing regime on the mechanical properties of ultra-high performance fibre reinforced concrete (UHPFRC). *Constr. Build. Mater.* **2009**, *23*, 2291–2298. [CrossRef]

96. Van, V.T.A.; Rößler, C.; Bui, D.D.; Ludwig, H.M. Rice husk ash as both pozzolanic admixture and internal curing agent in ultra-high performance concrete. *Cem. Concr. Compos.* **2014**, *53*, 270–278. [CrossRef]

97. Yoo, D.Y.; Banthia, N. Mechanical properties of ultra-high-performance fiber-reinforced concrete: A review. *Cem. Concr. Compos.* **2016**, *73*, 267–280. [CrossRef]

98. Ahmad, S.; Hakeem, I.; Maslehuddin, M. Development of UHPC mixtures utilizing natural and industrial waste materials as partial replacements of silica fume and sand. *Sci. World J.* **2014**, *2014*, 1–8. [CrossRef] [PubMed]

99. Li, Z. Drying shrinkage prediction of paste containing meta-kaolin and ultrafine fly ash for developing ultra-high performance concrete. *Mater. Today Commun.* **2016**, *6*, 74–80. [CrossRef]

100. Kim, H.; Koh, T.; Pyo, S. Enhancing flowability and sustainability of ultra high performance concrete incorporating high replacement levels of industrial slags. *Constr. Build. Mater.* **2016**, *123*, 153–160. [CrossRef]

101. Van Tuan, N.; Ye, G.; Van Breugel, K. Effect of rice husk ash on autogenous shrinkage of ultra high performance concrete. In Proceedings of the International RILEM Conference on Use of Superabsorbent Polymers and Other New Additives in Concrete, Lyngby, Denmark, 15–18 August 2010.

102. Schießl, P.; Mazanec, O.; Lowke, D. *SCC and UHPC-Effect of Mixing Technology on Fresh Concrete Properties*; Springer: Berlin/Heidelberg, Germany, 2007.

103. Yigiter, H.; Aydin, S.; Yazici, H.; Yardimci, M.Y. Mechanical performance of low cement reactive powder concrete (LCRPC). *Compos. B Eng.* **2012**, *43*, 2907–2914. [CrossRef]

104. Lee, N.K.; Koh, K.T.; Park, S.H.; Ryu, G.S. Microstructural investigation of calcium aluminate cement-based ultra-high performance concrete (UHPC) exposed to high temperatures. *Cem. Concr. Res.* **2017**, *102*, 109–118. [CrossRef]

105. Randl, N.; Steiner, T.; Ofner, S.; Baumgartner, E.; Mészöly, T. Development of UHPC mixtures from an ecological point of view. *Constr. Build. Mater.* **2014**, *67*, 373–378. [CrossRef]

106. Sharma, R.; Jang, J.G.; Bansal, P.P. A comprehensive review on effects of mineral admixtures and fibers on engineering properties of ultra-high-performance concrete. *J. Build. Eng.* **2022**, *45*, 103314. [CrossRef]

107. Yalçınkaya, Ç.; Çopuroğlu, O. Hydration heat, strength and microstructure characteristics of UHPC containing blast furnace slag. *J. Build. Eng.* **2021**, *34*, 101915. [CrossRef]

108. Mousavinejad, S.H.G.; Sammak, M. Strength and chloride ion penetration resistance of ultra-high-performance fiber reinforced geopolymer concrete. *Structures* **2021**, *32*, 1420–1427. [CrossRef]

109. Alsalman, A.; Dang, C.N.; Martí-Vargas, J.R.; Micah Hale, W. Mixture-proportioning of economical UHPC mixtures. *J. Build. Eng.* **2020**, *27*, 100970. [CrossRef]

110. Ganesh, P.; Murthy, A.R. Tensile behaviour and durability aspects of sustainable ultra-high performance concrete incorporated with GGBS as cementitious material. *Constr. Build. Mater.* **2019**, *197*, 667–680. [CrossRef]

111. Nadiger, A.; Madhavan, M.K. Influence of Mineral Admixtures and Fibers on Workability and Mechanical Properties of Reactive Powder Concrete. *J. Mater. Civ. Eng.* **2019**, *31*, 04018394. [CrossRef]

112. Vigneshwari, M.; Arunachalam, K.; Angayarkanni, A. Replacement of silica fume with thermally treated rice husk ash in Reactive Powder Concrete. *J. Clean. Prod.* **2018**, *188*, 264–277. [CrossRef]

113. Bahedh, M.A.; Jaafar, M.S. Ultra high-performance concrete utilizing fly ash as cement replacement under autoclaving technique. *Case Stud. Constr. Mater.* **2018**, *9*, e00202. [CrossRef]

114. Zhang, J.; Zhao, Y.; Li, H. Experimental Investigation and Prediction of Compressive Strength of Ultra-High Performance Concrete Containing Supplementary Cementitious Materials. *Adv. Mater. Sci. Eng.* **2017**, *2017*, 1–8. [CrossRef]

115. Huang, W.; Kazemi-Kamyab, H.; Sun, W.; Scrivener, K. Effect of replacement of silica fume with calcined clay on the hydration and microstructural development of eco-UHPFRC. *Mater. Des.* **2017**, *121*, 36–46. [CrossRef]

116. Ferdosian, I.; Camões, A.; Ribeiro, M. High-Volume Fly Ash Paste for Developing Ultra-High Performance Concrete (UHPC). *Ciênc. Tecnol. Mater.* **2017**, *29*, 157–161. [CrossRef]

117. Azreen, N.M.; Rashid, R.S.M.; Mugahed Amran, Y.H.; Voo, Y.L.; Haniza, M.; Hairie, M.; Alyousef, R.; Alabduljabbar, H. Simulation of ultra-high-performance concrete mixed with hematite and barite aggregates using Monte Carlo for dry cask storage. *Constr. Build. Mater.* **2020**, *263*, 120161. [CrossRef]

118. Yu, Z.; Wu, L.; Yuan, Z.; Zhang, C.; Bangi, T. Mechanical properties, durability and application of ultra-high-performance concrete containing coarse aggregate (UHPC-CA): A review. *Constr. Build. Mater.* **2022**, *334*, 127360. [CrossRef]

119. *ASTM C109*; Standard Test Method for Compressive Strength of Hydraulic Cement Mortars (Using 2-in. or [50-mm] Cube Specimens). ASTM: West Conshohocken, PA, USA, 2023.

120. *ASTM C39*; Standard Test Method for Compressive Strength of Cylindrical Concrete Specimens. ASTM: West Conshohocken, PA, USA, 2023.

121. Chan, Y.W.; Chu, S.H. Effect of silica fume on steel fiber bond characteristics in reactive powder concrete. *Cem. Concr. Res.* **2004**, *34*, 1167–1172. [CrossRef]

122. Chen, Z.; Wang, X.; Ding, L.; Jiang, K.; Liu, X.; Liu, J.; Wu, Z. Spalling resistance and mechanical properties of ultra-high performance concrete reinforced with multi-scale basalt fibers and hybrid fibers under elevated temperature. *J. Build. Eng.* **2023**, *77*, 107435. [CrossRef]

123. Bărbos, G.A. What Makes Ultra-High Performance Concrete (Uhpc) a Special Material? In *Lucrările Conferinţei de Cercetare în Construcţii, Economia Construcţiilor, Urbanism şi Amenajarea Teritoriului*; INCD URBAN-INCERC: București, Romania, 2023; pp. 77–84.

124. Alkadhim, H.A.; Amin, M.N.; Ahmad, W.; Khan, K.; Umbreen-us-Sahar; Al-Hashem, M.N.; Mohamed, A. An overview of progressive advancement in ultra-high performance concrete with steel fibers. *Front. Mater.* **2022**, *9*, 1091867. [CrossRef]

125. Bede Odorčić, N.; Kravanja, G. Combined Effects of Metakaolin and Hybrid Fibers on Self-Compacting Concrete. *Materials* **2022**, *15*, 5588. [CrossRef]

126. Rizwan Mumtaz, A.; Bede Odorčić, N.; Garro, N.; Lubej, S.; Ivanič, A.; Comite, A.; Pagliero, M.; Kravanja, G. Novel Ultra-High-Performance Concrete (UHPC) Enhanced by Superhydrophobic and Self-Luminescent Features. *Sustainability* **2024**, *16*, 1068. [CrossRef]

127. Zhong, X.; Hu, H.; Yang, L.; Sheng, J.; Fu, H. Robust Hyperbranched Polyester-Based Anti-Smudge Coatings for Self-Cleaning, Anti-Graffiti, and Chemical Shielding. *ACS Appl. Mater. Interfaces* **2019**, *11*, 14305–14312. [CrossRef]

128. Azreen, N.M.; Rashid, R.S.M.; Haniza, M.; Voo, Y.L.; Mugahed Amran, Y.H. Radiation shielding of ultra-high-performance concrete with silica sand, amang and lead glass. *Constr. Build. Mater.* **2018**, *172*, 370–377. [CrossRef]

129. Zelić, J.; Rušić, D.; Veža, D.; Krstulović, R. Role of silica fume in the kinetics and mechanisms during the early stage of cement hydration. *Cem. Concr. Res.* **2000**, *30*, 1655–1662. [CrossRef]

130. Yang, J.; Chen, B.; Wu, X.; Xu, G. Quantitative analysis of steel fibers on UHPFRC uniaxial tensile behavior using X-CT and UTT. *Constr. Build. Mater.* **2023**, *368*, 130349. [CrossRef]

131. Wang, W.; Sha, A.; Lu, Z.; Jia, M.; Jiang, W.; Liu, Z.; Yuan, D. Self-luminescent cement-based composite materials: Properties and mechanisms. *Constr. Build. Mater.* **2021**, *269*, 121267. [CrossRef]

132. Ribbing, C. Environmentally Friendly Use of Non-Coal Ashes in Sweden. *Waste Manag.* **2007**, *27*, 1428–1435. [CrossRef] [PubMed]

133. El-Tawil, S.; Tai, Y.S.; Meng, B.; Hansen, W.; Liu, Z. *Commercial Production of Non-Proprietary Ultra High Performance Concrete (No. RC-1670)*; Michigan Department of Transportation: Lansing, MI, USA, 2018.

134. Wille, K.; El-Tawil, S.; Naaman, A.E. Properties of strain hardening ultra high performance fiber reinforced concrete (UHP-FRC) under direct tensile loading. *Cem. Concr. Compos.* **2014**, *48*, 53–66. [CrossRef]

135. Denarié, E.; Brühwiler, E. Strain-Hardening Ultra-High Performance Fibre Reinforced Concrete: Deformability versus Strength Optimization. *Restor. Build. Monuments* **2011**, *17*, 397–410. [CrossRef]

136. Muhd Norhasri, M.S.; Hamidah, M.S.; Mohd Fadzil, A.; Megawati, O. Inclusion of nano metakaolin as additive in ultra high performance concrete (UHPC). *Constr. Build. Mater.* **2016**, *127*, 167–175. [CrossRef]

137. Al-Rousan, E.T.; Khalid, H.R.; Rahman, M.K. Fresh, mechanical, and durability properties of basalt fiber-reinforced concrete (BFRC): A review. *Dev. Built Environ.* **2023**, *14*, 100155. [CrossRef]

138. Larissa, L.C.; Marcos, M.A.; Maria, M.V.; de Souza, N.S.L.; de Farias, E.C. Effect of high temperatures on self-compacting concrete with high levels of sugarcane bagasse ash and metakaolin. *Constr. Build. Mater.* **2020**, *248*, 118715.

139. Özkan, Ş.; Demir, F. The hybrid effects of PVA fiber and basalt fiber on mechanical performance of cost effective hybrid cementitious composites. *Constr. Build. Mater.* **2020**, *263*, 120564. [CrossRef]

140. Xu, X.; Cui, S.; Cao, Z.; Zhang, S.; Woody Ju, J.W.; Liu, P.; Wang, X. Study on the interfacial bonding performance of basalt ultra-high performance concrete repair and reinforcement materials under severe service environment. *Constr. Build. Mater.* **2023**, *400*, 132624. [CrossRef]

141. Xie, H.; Wei, P.; Liu, N.; Gao, J.; Yang, L.; Li, J.; Chen, S. Study on failure characteristics of basalt fiber reactive powder concrete under uniaxial loading. *Constr. Build. Mater.* **2023**, *404*, 133246. [CrossRef]

142. Ziada, M.; Erdem, S.; Tammam, Y.; Kara, S.; Lezcano, R.A.G. The effect of basalt fiber on mechanical, microstructural, and high-temperature properties of fly ash-based and basalt powder waste-filled sustainable geopolymer mortar. *Sustainability* **2021**, *13*, 12610. [CrossRef]

143. Han, B.; Zhang, L.; Jinping, O. *Smart and Multifunctional Concrete toward Sustainable Infrastructures*; Springer: Singapore, 2018.

144. Elnaggar, E.M.; Elsokkary, T.M.; Shohide, M.A.; El-Sabbagh, B.A.; Abdel-Gawwad, H.A. Surface protection of concrete by new protective coating. *Constr. Build. Mater.* **2019**, *220*, 245–252. [CrossRef]

145. Guo, T.; Weng, X. Evaluation of the freeze-thaw durability of surface-treated airport pavement concrete under adverse conditions. *Constr. Build. Mater.* **2019**, *206*, 519–530. [CrossRef]

146. Habibnejad Korayem, A.; Ghoddousi, P.; Shirzadi Javid, A.A.; Oraie, M.A.; Ashegh, H. Graphene oxide for surface treatment of concrete: A novel method to protect concrete. *Constr. Build. Mater.* **2020**, *243*, 118229. [CrossRef]

147. Zheng, W.; Chen, W.G.; Feng, T.; Li, W.Q.; Liu, X.T.; Dong, L.L.; Fu, Y.Q. Enhancing chloride ion penetration resistance into concrete by using graphene oxide reinforced waterborne epoxy coating. *Prog. Org. Coat.* **2020**, *138*, 105389. [CrossRef]

148. Tam, C.M.; Tam, V.W.Y.; Ng, K.M. Assessing drying shrinkage and water permeability of reactive powder concrete produced in Hong Kong. *Constr. Build. Mater.* **2012**, *26*, 79–89. [CrossRef]

149. Pan, X.; Shi, Z.; Shi, C.; Ling, T.C.; Li, N. A review on concrete surface treatment Part I: Types and mechanisms. *Constr. Build. Mater.* **2017**, *132*, 578–590. [CrossRef]

150. Li, J.; Wu, Z.; Shi, C.; Yuan, Q.; Zhang, Z. Durability of ultra-high performance concrete—A review. *Constr. Build. Mater.* **2020**, *255*, 119296. [CrossRef]

151. Tittarelli, F.; Moriconi, G. Comparison between surface and bulk hydrophobic treatment against corrosion of galvanized reinforcing steel in concrete. *Cem. Concr. Res.* **2011**, *41*, 609–614. [CrossRef]

152. Basheer, P.A.M.; Basheer, L.; Cleland, D.J.; Long, A.E. Surface Treatments for Concrete: Assessmentmethods and Reported Performance. *Constr. Build. Mater.* **1997**, *11*, 413–429. [CrossRef]

153. De Vries, I.J.; Polder, R.B. Hydrophobic Treatment of Concrete. *Constr. Build. Mater.* **1997**, *11*, 259–265. [CrossRef]

154. Tittarelli, F. Oxygen diffusion through hydrophobic cement-based materials. *Cem. Concr. Res.* **2009**, *39*, 924–928. [CrossRef]

155. Gao, Y.; Qu, L.; He, B.; Dai, K.; Fang, Z.; Zhu, R. Study on effectiveness of anti-icing and deicing performance of super-hydrophobic asphalt concrete. *Constr. Build. Mater.* **2018**, *191*, 270–280. [CrossRef]

156. Lv, L.; Zhao, W.; Zhong, X.; Fu, H. Fabrication of Magnetically Inorganic/Organic Superhydrophobic Fabrics and Their Applications. *ACS Appl. Mater. Interfaces* **2020**, *12*, 45296–45305. [CrossRef]

157. Sakr, M.R.; Bassuoni, M.T. Silane and methyl-methacrylate based nanocomposites as coatings for concrete exposed to salt solutions and cyclic environments. *Cem. Concr. Compos.* **2021**, *115*, 103841. [CrossRef]

158. Wei, Q.; Liu, X.; Zhang, X. Facile preparation of mechanically robust superhydrophobic concrete with self-cleaning property. *Mater. Res. Express* **2019**, *6*, 015001. [CrossRef]

159. Ong, J.; Zhao, D.; Han, Z.; Xu, W.; Lu, Y.; Liu, X.; Liu, B.; Carmalt, C.J.; Deng, X.; Parkin, I.P. Super-Robust Superhydrophobic Concrete. *J. Mater. Chem. A* **2017**, *5*, 14542–14550.

160. Kravanja, G.; Godec, R.F.; Rozman, M.; Rudolf, R.; Ivanič, A. Biomimetic Superhydrophobic Concrete with Enhanced Anticorrosive, Freeze Thaw, and Deicing Resistance. *Adv. Eng. Mater.* **2022**, *24*, 2101445. [CrossRef]

161. Chen, P.-W.; Chung, D.D.L. Carbon Fiber Reinforced Concrete for Smart Structures Capable of Non-Destructive Flaw Detection. *Smart Mater. Struct.* **1993**, *2*, 22–30. [CrossRef]

162. Guo, Y.; Li, W.; Dong, W.; Wang, K.; He, X.; Vessalas, K.; Sheng, D. Self-sensing cement-based sensors with superhydrophobic and self-cleaning capacities after silane-based surficial treatments. *Case Stud. Constr. Mater.* **2022**, *17*, e01311. [CrossRef]

163. Ding, S.; Dong, S.; Wang, X.; Ding, S.; Han, B.; Ou, J. Self-heating ultra-high performance concrete with stainless steel wires for active deicing and snow-melting of transportation infrastructures. *Cem. Concr. Compos.* **2023**, *138*, 105005. [CrossRef]

164. Peña-García, A. The impact of lighting on drivers well-being and safety in very long underground roads: New challenges for new infrastructures. *Tunn. Undergr. Space Technol.* **2018**, *80*, 38–43. [CrossRef]

165. Voravanicha, K.; Leelachao, S.; Sahasithiwat, S.; Kumnorkaew, P.; Dangtungee, R. Natural Rubber Filled with Phosphorescent Materials for Pavement. *Mater. Today* **2019**, *17*, 1971–1976. [CrossRef]

166. Zhu, C.; Lv, J.; Chen, L.; Lin, W.; Zhang, J.; Yang, J.; Feng, J. Dark, heat-reflective, anti-ice rain and superhydrophobic cement concrete surfaces. *Constr. Build. Mater.* **2019**, *220*, 21–28. [CrossRef]

167. Konarzewska, B. Smart Materials in Architecture: Useful Tools with Practical Applications or Fascinating Inventions for Experimental Design? *IOP Conf. Ser. Mater. Sci. Eng.* **2017**, *245*, 052098. [CrossRef]

168. Sha, A.; Liu, Z.; Jiang, W.; Qi, L.; Hu, L.; Jiao, W.; Barbieri, D.M. Advances and development trends in eco-friendly pavements. *J. Road Eng.* **2021**, *1*, 1–42. [CrossRef]

169. Tayeh, B.A.; Abu Bakar, B.H.; Megat Johari, M.A.; Voo, Y.L. Mechanical and permeability properties of the interface between normal concrete substrate and ultra high performance fiber concrete overlay. *Constr. Build. Mater.* **2012**, *36*, 538–548. [CrossRef]
170. Ghafari, E.; Costa, H.; Júlio, E.; Portugal, A.; Durães, L. The effect of nanosilica addition on flowability, strength and transport properties of ultra high performance concrete. *Mater. Des.* **2014**, *59*, 1–9. [CrossRef]
171. Chuang, M.L.; Huang, W.H. Durability Analysis Testing on Reactive Powder Concrete. *Adv. Mat. Res.* **2013**, *811*, 244–248. [CrossRef]
172. Liu, J.; Song, S.; Wang, L. Durability and micro-structure of reactive powder concrete. *J. Wuhan Univ. Technol. Mater. Sci. Ed.* **2009**, *24*, 506–509. [CrossRef]
173. Roux, N.; Andrade, C.; Sanjuan, M.A. Experimental Study of Durability of Reactive Powder Concretes. *J. Mater. Civ. Eng.* **1996**, *8*, 1–6. [CrossRef]
174. Ghafari, E.; Arezoumandi, M.; Costa, H.; Júlio, E. Influence of nano-silica addition in the durability of UHPC. *Constr. Build. Mater.* **2015**, *94*, 181–188. [CrossRef]
175. Bondar, D.; Lynsdale, C.J.; Milestone, N.B.; Hassani, N. Sulfate Resistance of Alkali Activated Pozzolans. *Int. J. Concr. Struct. Mater.* **2015**, *9*, 145–158. [CrossRef]
176. Mu, R.; Miao, C.; Luo, X.; Sun, W. Interaction between Loading, Freeze–Thaw Cycles, and Chloride Salt Attack of Concrete with and without Steel Fiber Reinforcement. *Cem. Concr. Res.* **2002**, *32*, 1061–1066. [CrossRef]
177. Peng, Y.; Zhang, J.; Liu, J.; Ke, J.; Wang, F. Properties and microstructure of reactive powder concrete having a high content of phosphorous slag powder and silica fume. *Constr. Build. Mater.* **2015**, *101*, 482–487. [CrossRef]
178. Dils, J.; Boel, V.; De Schutter, G. Influence of cement type and mixing pressure on air content, rheology and mechanical properties of UHPC. *Constr. Build. Mater.* **2013**, *41*, 455–463. [CrossRef]
179. Zhong, R.; Wille, K. Material design and characterization of high performance pervious concrete. *Constr. Build. Mater.* **2015**, *98*, 51–60. [CrossRef]
180. Sanchayan, S.; Foster, S.J. High temperature behaviour of hybrid steel–PVA fibre reinforced reactive powder concrete. *Mater. Struct./Mater. Constr.* **2016**, *49*, 769–782. [CrossRef]
181. Feylessoufi, A.; Crespin, M.; Dion, P.; Bergaya, F.; Van Damme, H.; Richard, P. Controlled Rate Thermal Treatment of Reactive Powder Concretes. *Adv. Cem. Based Mater.* **1997**, *6*, 21–27. [CrossRef]
182. Rajak, M.A.A.; Majid, Z.A.; Ismail, M. Morphological Characteristics of Hardened Cement Pastes Incorporating Nano-palm Oil Fuel Ash. *Procedia Manuf.* **2015**, *2*, 512–518. [CrossRef]
183. Alhassan, M.; Alkhawaldeh, A.; Betoush, N.; Alkhawaldeh, M.; Huseien, G.F.; Amaireh, L.; Elrefae, A. Life Cycle Assessment of the Sustainability of Alkali-Activated Binders. *Biomimetics* **2023**, *8*, 58. [CrossRef] [PubMed]
184. Luo, Z.; Zhi, T.; Liu, X.; Yin, K.; Pan, H.; Feng, H.; Song, Y.; Su, Y. Effects of different nanomaterials on the early performance of ultra-high performance concrete (UHPC): C–S–H seeds and nano-silica. *Cem. Concr. Compos.* **2023**, *142*, 105211. [CrossRef]
185. Zhang, A.; Yang, W.; Ge, Y.; Du, Y.; Liu, P. Effects of nano-SiO_2 and nano-Al_2O_3 on mechanical and durability properties of cement-based materials: A comparative study. *J. Build. Eng.* **2021**, *34*, 101936. [CrossRef]
186. Wu, Z.; Khayat, K.H.; Shi, C.; Tutikian, B.F.; Chen, Q. Mechanisms underlying the strength enhancement of UHPC modified with nano-SiO_2 and nano-$CaCO_3$. *Cem. Concr. Compos.* **2021**, *119*, 103992. [CrossRef]
187. Elrahman, M.A.; Chung, S.Y.; Sikora, P.; Rucinska, T.; Stephan, D. Influence of nanosilica on mechanical properties, sorptivity, and microstructure of lightweight concrete. *Materials* **2019**, *12*, 3078. [CrossRef]
188. Beigi, M.H.; Berenjian, J.; Lotfi Omran, O.; Sadeghi Nik, A.; Nikbin, I.M. An experimental survey on combined effects of fibers and nanosilica on the mechanical, rheological, and durability properties of self-compacting concrete. *Mater. Des.* **2013**, *50*, 1019–1029. [CrossRef]
189. Behzadian, R.; Shahrajabian, H. Experimental Study of the Effect of Nano-silica on the Mechanical Properties of Concrete/PET Composites. *KSCE J. Civ. Eng.* **2019**, *23*, 3660–3668. [CrossRef]
190. Hosan, A.; Shaikh, F.U.A. Influence of nano silica on compressive strength, durability, and microstructure of high-volume slag and high-volume slag–fly ash blended concretes. *Struct. Concr.* **2021**, *22*, E474–E487. [CrossRef]
191. Potapov, V.; Efimenko, Y.; Fediuk, R.; Gorev, D. Effect of hydrothermal nanosilica on the performances of cement concrete. *Constr. Build. Mater.* **2021**, *269*, 121307. [CrossRef]
192. Madandoust, R.; Mohseni, E.; Mousavi, S.Y.; Namnevis, M. An experimental investigation on the durability of self-compacting mortar containing nano-SiO_2, nano-Fe_2O_3 and nano-CuO. *Constr. Build. Mater.* **2015**, *86*, 44–50. [CrossRef]
193. Wang, L.; Zheng, D.; Zhang, S.; Cui, H.; Li, D. Effect of nano-$SiO2$ on the hydration and microstructure of Portland cement. *Nanomaterials* **2016**, *6*, 241. [CrossRef] [PubMed]
194. Saleh, N.J.; Ibrahim, R.I.; Salman, A.D. Characterization of nano-silica prepared from local silica sand and its application in cement mortar using optimization technique. *Adv. Powder Technol.* **2015**, *26*, 1123–1133. [CrossRef]
195. Kontoleontos, F.; Tsakiridis, P.E.; Marinos, A.; Kaloidas, V.; Katsioti, M. Influence of colloidal nanosilica on ultrafine cement hydration: Physicochemical and microstructural characterization. *Constr. Build. Mater.* **2012**, *35*, 347–360. [CrossRef]
196. Adak, D.; Sarkar, M.; Mandal, S. Structural performance of nano-silica modified fly-ash based geopolymer concrete. *Constr. Build. Mater.* **2017**, *135*, 430–439. [CrossRef]
197. Deb, P.S.; Sarker, P.K.; Barbhuiya, S. Sorptivity and acid resistance of ambient-cured geopolymer mortars containing nano-silica. *Cem. Concr. Compos.* **2016**, *72*, 235–245. [CrossRef]

198. Phoo-ngernkham, T.; Chindaprasirt, P.; Sata, V.; Hanjitsuwan, S.; Hatanaka, S. The effect of adding nano-SiO_2 and nano-Al_2O_3 on properties of high calcium fly ash geopolymer cured at ambient temperature. *Mater. Des.* **2014**, *55*, 58–65. [CrossRef]

199. Revathy, J.; Gajalakshmi, P.; Aseem Ahmed, M. Flowable Nano SiO_2 Based Cementitious Mortar for Ferrocement Jacketed Column. *Mater. Today* **2020**, *22*, 836–842. [CrossRef]

200. Palla, R.; Karade, S.R.; Mishra, G.; Sharma, U.; Singh, L.P. High strength sustainable concrete using silica nanoparticles. *Constr. Build. Mater.* **2017**, *138*, 285–295. [CrossRef]

201. Zhang, M.H.; Islam, J. Use of nano-silica to reduce setting time and increase early strength of concretes with high volumes of fly ash or slag. *Constr. Build. Mater.* **2012**, *29*, 573–580. [CrossRef]

202. Najafi Kani, E.; Rafiean, A.H.; Alishah, A.; Hojjati Astani, S.; Ghaffar, S.H. The effects of Nano-Fe_2O_3 on the mechanical, physical and microstructure of cementitious composites. *Constr. Build. Mater.* **2021**, *266*, 121137. [CrossRef]

203. Huseien, G.F.; Hamzah, H.K.; Mohd Sam, A.R.; Khalid, N.H.A.; Shah, K.W.; Deogrescu, D.P.; Mirza, J. Alkali-activated mortars blended with glass bottle waste nano powder: Environmental benefit and sustainability. *J. Clean. Prod.* **2020**, *243*, 118636. [CrossRef]

204. Ma, B.; Li, H.; Mei, J.; Li, X.; Chen, F. Effects of nano-TiO_2 on the toughness and durability of cement-based material. *Adv. Mater. Sci. Eng.* **2015**, *2015*, 583106. [CrossRef]

205. Duan, P.; Yan, C.; Luo, W.; Zhou, W. Effects of adding nano-TiO_2 on compressive strength, drying shrinkage, carbonation and microstructure of fluidized bed fly ash based geopolymer paste. *Constr. Build. Mater.* **2016**, *106*, 115–125. [CrossRef]

206. Idrees, M.; Saeed, F.; Amin, A.; Hussain, T. Improvement in compressive strength of Styrene-Butadiene-Rubber (SBR) modified mortars by using powder form and nanoparticles. *J. Build. Eng.* **2021**, *44*, 102651. [CrossRef]

207. Mirgozar Langaroudi, M.A.; Mohammadi, Y. Effect of nano-clay on workability, mechanical, and durability properties of self-consolidating concrete containing mineral admixtures. *Constr. Build. Mater.* **2018**, *191*, 619–634. [CrossRef]

208. Mohseni, E.; Khotbehsara, M.M.; Naseri, F.; Monazami, M.; Sarker, P. Polypropylene fiber reinforced cement mortars containing rice husk ash and nano-alumina. *Constr. Build. Mater.* **2016**, *111*, 429–439. [CrossRef]

209. Praveenkumar, T.R.; Vijayalakshmi, M.M.; Meddah, M.S. Strengths and durability performances of blended cement concrete with TiO_2 nanoparticles and rice husk ash. *Constr. Build. Mater.* **2019**, *217*, 343–351. [CrossRef]

210. Abbasi, S.M.; Ahmadi, H.; Khalaj, G.; Ghasemi, B. Microstructure and mechanical properties of a metakaolinite-based geopolymer nanocomposite reinforced with carbon nanotubes. *Ceram. Int.* **2016**, *42*, 15171–15176. [CrossRef]

211. Wang, L.; Zhang, H.; Gao, Y. Effect of TiO_2 nanoparticles on physical and mechanical properties of cement at low temperatures. *Adv. Mater. Sci. Eng.* **2018**, *2018*, 8934689. [CrossRef]

212. Nazari, A.; Riahi, S. Improvement compressive strength of concrete in different curing media by Al_2O_3 nanoparticles. *Mater. Sci. Eng. A* **2011**, *528*, 1183–1191. [CrossRef]

213. Zhang, M.H.; Li, H. Pore structure and chloride permeability of concrete containing nano-particles for pavement. *Constr. Build. Mater.* **2011**, *25*, 608–616. [CrossRef]

214. Shekari, A.H.; Razzaghi, M.S. Influence of nano particles on durability and mechanical properties of high performance concrete. *Procedia Eng.* **2011**, *14*, 3036–3041. [CrossRef]

215. Kishore, K.; Pandey, A.; Wagri, N.K.; Saxena, A.; Patel, J.; Al-Fakih, A. Technological challenges in nanoparticle-modified geopolymer concrete: A comprehensive review on nanomaterial dispersion, characterization techniques and its mechanical properties. *Case Stud. Constr. Mater.* **2023**, *19*, e02265. [CrossRef]

216. Dong, Y. Performance assessment and design of ultra-high performance concrete (UHPC) structures incorporating life-cycle cost and environmental impacts. *Constr. Build. Mater.* **2018**, *167*, 414–425. [CrossRef]

217. Steinberg, E. Structural Reliability of Prestressed UHPC Flexure Models for Bridge Girders. *ASCE* **2009**, *15*, 65–72. [CrossRef]

218. Kim, S.; Frangopol, D.M. Probabilistic bicriterion optimum inspection/monitoring planning: Applications to naval ships and bridges under fatigue. *Struct. Infrastruct. Eng.* **2012**, *8*, 912–927.

219. García-Segura, T.; Yepes, V.; Alcalá, J. Life cycle greenhouse gas emissions of blended cement concrete including carbonation and durability. *Int. J. Life Cycle Assess.* **2014**, *19*, 3–12. [CrossRef]

220. Bouhaya, L.; Le Roy, R.; Feraille-Fresnet, A. Simplified environmental study on innovative bridge structure. *Environ. Sci. Technol.* **2009**, *43*, 2066–2071. [CrossRef] [PubMed]

221. Mohammed Safi, H.S.R.K.; George, R. Development of the Swedish bridge management system by upgrading and expanding the use of LCC. *Struct. Infrastruct. Eng.* **2013**, *9*, 1240–1250. [CrossRef]

222. Jones, T.W.; Smith, D. An Historical Perspective of Net Present Value and Equivalent Annual Cost. *Account. Hist. J.* **1982**, *9*, 103–110. [CrossRef]

223. Kauffmann, P.; Howard, E.; Yao, J.; Harbinson, D.; Brooks, N.; Williams, R.; Gurganus, C. Criteria for fleet management. *Transp. Res. Rec.* **2012**, *2292*, 171–178. [CrossRef]

224. Chu, H.; Wang, F.; Wang, L.; Feng, T.; Wang, D. Mechanical properties and environmental evaluation of ultra-high-performance concrete with aeolian sand. *Materials* **2020**, *13*, 3148. [CrossRef]

225. Kien, T.T. Comparison of energy consumption, CO_2 emissions between normal concrete and UHPC in rural bridge application. *J. Sci. Technol. Civ. Eng.* **2023**, *17*, 168–179. [CrossRef]

226. Mazzacane, P.; Ricciotti, R.; Teply, F.; Tollini, E.; Corvez, D. Mucem: The Builder's Perspective. In Proceedings of the RILEM-fib-AFGC International Symposium on Ultra-High Performance Fibre-Reinforced Concrete, Marseille, France, 1–3 October 2013.

227. Aubry, S.; Bompas, P.; Vaudeville, B.; Corvez, D.; Lagrange, T.; Mazzacane, P.; Brizou, A. A UHPFRC Cladding Challenge: The Fondation Louis Vuitton Pour La Création. In Proceedings of the RILEM-fib-AFGC International Symposium on Ultra-High Performance Fibre-Reinforced Concrete, Marseille, France, 1–3 October 2013.

228. Muttoni, A.; Brauen, U.; Jaquier, J.L.; Moullet, D. A New Roof for the Olympic Museum At. In Proceedings of the International Symposium on Ultra-High Performance Fiber-Reinforced Concrete, Marseille, France, 1–3 October 2013.

229. Russell, H.G.; Graybeal, B.A.; Russell, H.G. *Ultra-High Performance Concrete: A State-of-the-Art Report for the Bridge Community (No. FHWA-HRT-13-060)*; Federal Highway Administration, Office of Infrastructure Research and Development: Washington, DC, USA, 2013.

230. Akhnoukh, A.K.; Buckhalter, C. Ultra-high-performance concrete: Constituents, mechanical properties, applications and current challenges. *Case Stud. Constr. Mater.* **2021**, *15*, e00559. [CrossRef]

231. Prabhu, S.; Prakash, K.B.; Shashishankar, A.; Mahdi, S.N.; Mohiyuddin, C.S. Green approach on ternary blended pre stressed cement concrete railway sleepers. *Clean. Mater.* **2022**, *4*, 100079. [CrossRef]